Spatial patterns in glacier characteristics and area changes from 1962 to 2006 in the Kanchenjunga-Sikkim area, eastern Himalaya

Adina E. Racoviteanu[1,*], Y. Arnaud[1,2], Mark W. Williams[3] and William F. Manley[4]

[1]Laboratoire de Glaciologie et Géophysique de l'Environnement, 54, rue Molière, Domaine Universitaire, BP 96 38402 Saint Martin d'Hères cedex, France
[2]Laboratoire d'Étude des Transferts en Hydrologie et Environnement, BP 53 38401 Saint Martin d'Hères cedex, France
[3]Department of Geography and Institute of Arctic and Alpine Research, University of Colorado, Boulder CO 80309
[4]Institute of Arctic and Alpine Research, University of Colorado, Boulder CO 80309

* *Correspondence to:* Adina Racoviteanu (racovite@gmail.com)

Abstract

This study investigates spatial patterns in glacier characteristics and area changes at decadal scales in the eastern Himalaya: Nepal (Arun and Tamor basins), India (Tista basin in Sikkim), and parts of China and Bhutan based on various satellite imagery: Corona KH4 imagery, Landsat 7 Enhanced Thematic Mapper Plus (ETM+) and Advanced Spaceborne Thermal Emission Radiometer (ASTER), QuickBird (QB) and WorldView-2 (WV2). We compare and contrast glacier surface area changes 1962 – 2000/2006 and their dependency on glacier topography (elevation, slope, aspect, percent debris cover), climate (solar radiation and precipitation) on the eastern side (Sikkim) versus the western side (Nepal).

Glacier mapping from 2000 Landsat ASTER yielded 1,463 ± 88 km^2 total glacierized area, of which 569 ± 34 km^2 was located in Sikkim and 488 ± 29 km^2 in eastern Nepal. Supraglacial debris covered 11% of the total glacierized area, and supraglacial lakes

covered about 5.8% of the debris-covered glacier area. Glacier area change (1962 to 2000) was -0.50 ± 0.2% yr^{-1}, with little difference between Nepal (0.53 ± 0.2% yr^{-1}) and Sikkim (0.44 ± 0.2% yr^{-1}). Glacier area change was controlled mostly by glacier area, elevation, altitudinal range and to a smaller extent slope and aspect. In the Kanchenjunga-Sikkim area, we estimated a glacier area change of -0.23 ± 0.08% yr^{-1} from 1962 to 2006 based on high-resolution imagery. On a glacier-by-glacier basis, clean glaciers exhibit more area loss on average from 1962 to 2006 (34%) compared to debris-covered glaciers (22%). Glaciers in this region of the Himalaya area are shrinking at similar rates to those reported for the last decades in other parts of the Himalaya, but individual glacier rates of change vary across the study area with respect to local topography, percent debris cover or glacier elevations.

1. Introduction

Himalayan glaciers have generated a lot of concern in the last few years, particularly with respect to potential consequences of glacier changes on the regional water cycle (Kaser et al., 2010; Immerzeel et al., 2012; Immerzeel et al., 2010; Racoviteanu et al., 2013a). In the last decades, the availability of low-cost data from optical remote sensing platforms with global coverage provided opportunities for glacier mapping at regional scales. Remote sensing techniques have helped improve estimates of glacier area changes (Bhambri et al., 2010; Bolch, 2007; Bajracharya et al., 2007; Kamp et al., 2011; Bolch et al., 2008a), glacier lake changes (Bajracharya et al., 2007; Bolch et al., 2008b; Gardelle et al., 2011; Wessels et al., 2002) and region-wide glacier mass balance (Berthier et al., 2007; Bolch et al., 2011; Gardelle et al., 2013; Kääb et al., 2012), but significant gaps do remain. The new global Randolph Glacier Inventory (RGI) v.4 (Pfeffer et al., 2014)

provides a global dataset of glacier outlines intended for large-scale studies; however, in some regions the quality varies, and the outlines may not be suitable for detailed regional analysis of glacier parameters. A new Landsat-based inventory has been complied using imagery from 1999 to 2003, which along with the current study, may help improve the accuracy in some areas of RGI (Nuimura et al., 2014). Some other regional glacier inventories have been constructed in the past, for example for the western part of the Himalaya (e.g. Kamp et al., 2011; Bhambri et al., 2011; Frey et al., 2012), but only a few are available for the eastern extremity of the Himalaya (e.g. Krishna, 2005; Bahuguna, 2001; Basnett et al., 2013; Bajracharya and Shrestha, 2011). The use of remote sensing for glacier mapping in this area is limited by frequent cloud cover and sensor saturation due to unsuitable gain settings and the persistence of seasonal snow, which hampers quality satellite image acquisition. Furthermore, this area has very limited reliable baseline topographic data needed for glacier change detection, as discussed in detail in Bhambri and Bolch (2009). The earliest Indian glacier maps date from topographic surveys conducted by expeditions in the mid-nineteenth century (Mason, 1954), but these are limited to a few glaciers. The Geologic Survey of India (GSI) inventory based on 1970s Survey of India maps (Sangewar and Shukla, 2009; Shanker, 2001) is not in the public domain. For eastern Nepal, 1970's topographic maps from Survey of India 1:63,000 scale are available, but their accuracy is not known with certainty. Given these limitations, declassified Corona imagery from the 1960's and 1970's has increasingly been used to develop baseline glacier datasets, for example in the Tien Shan (Narama et al., 2010), Nepal Himalaya (Bolch et al., 2008a) and parts of Sikkim Himalaya (Raj et al., 2013).

The topographic and climatic controls on glacier surface area have received increasing attention in recent studies, particularly with respect to debris-covered glaciers (Basnett et al., 2013; Thakuri et al., 2014; Bolch et al., 2008a; Salerno et al., 2008). Some studies have characterized the small-scale glacier surface topography of debris-covered glaciers using field-based surveys (Iwata et al., 2000; Sakai and Fujita, 2010; Zhang et al., 2011), while other studies focused on understanding patterns at the mountain-range scale (Scherler et al., 2011; Bolch et al., 2012; Gardelle et al., 2013; Racoviteanu et al., 2014). Glacier shrinkage and mass loss has been documented in the Himalaya concomitantly with an increase in debris cover (Bolch et al., 2011; Nuimura et al., 2012). However, the influence of debris cover on glacier mass balance remains debatable (Scherler et al., 2011; Kääb et al., 2012), and modeling of melt under the debris cover is subject to uncertainties due to limited field-based measurements of debris thickness needed for model parameterization (Zhang et al., 2011; Foster et al., 2012; Mihalcea et al., 2008b; Mihalcea et al., 2008a).

While significant progress has been made in the recent years on remote sensing glacier mapping in the Himalaya, some of the sub-regions still need updated glacier area and surface characteristics including debris cover. The objective of this study is two-fold: (1) present the current glacier distribution and characteristics in a data-scare area of the eastern Himalaya based on an updated 2000 Landsat ETM+ and ASTER inventory, along with elevation data from the Shuttle Radar Topography Mission (SRTM); (2) investigate spatial patterns in glacier surface area changes from 1962 (Corona KH4) to 2000 (Landsat/ASTER) and 2006 (QB) 2006 (WV2) and their dependence on topographic and climatic factors, with a particular emphasis on debris-covered glacier tongues. These

updated glacier datasets help fill a gap in global glacier inventories such as the RGI (Pfeffer et al., 2014), as well as for subsequent future mass balance applications at regional scales.

2. Study area

The study area encompasses glaciers in the eastern Himalaya (27° 04' 52" N to 28° 08' 26" N latitude and 88° 00' 57" E to 88° 55' 50" E longitude), located on either side of the border between Nepal and India in the Kanchenjunga-Sikkim area (Fig. 1). Based on SRTM data, relief in this area ranges from 300 m at the bottom of the valleys to 8,598 m (Mt. Kanchenjunga). Valley glaciers cover about 68% of the glacierized area, mountain glaciers cover 28%, and the remaining are cirque glaciers and aprons (Mool et al., 2002). The glacier ablation area is typically covered by heavy debris-cover originating from rockfall on the steep slopes (Mool et al., 2002), reaching up to a thickness of several meters at the glacier termini (Kayastha et al., 2000). The eastern part of this area constitutes the Sikkim province of India, and the western part is located in eastern Nepal, and encompasses the Tamor and parts of Arun basin. Climatically, this area of the Himalaya is dominated by the South Asian summer monsoon circulation system (Bhatt and Nakamura, 2005), caused by the inflow of moist air from the Bay of Bengal to the Indian subcontinent during the summer (Benn and Owen, 1998; Yanai et al., 1992). The Himalaya and Tibetan plateau (HTP) acts as a barrier to the monsoon winds, bringing about 77% of precipitation on the south slopes of the Himalaya during the summer months (May to September) (Fig. 2). This climatic particularity causes a "summer-accumulation" glacier regime type, with accumulation and ablation occurring simultaneously in the summer (Ageta and Higuchi, 1984). In Sikkim, rainfall amounts

range from 500 to 5000 mm per year, with annual averages of 3,580 mm recorded at Gangtok station (1,812 m) (1951 to 1980) (IMD, 1980), and 164 rainy days per year (Nandy et al., 2006). Mean minimum and maximum daily temperatures at Gangtok station were reported as 11.3°C and 19.8°C, with an average of 15.5°C based on the same observation record (IMD, 1980).

[Fig. 1 – 2]

3. Methodology

3.1. Data sources

Satellite imagery

Remote sensing datasets used in this study are summarized in Table 1, and included: 1) baseline remote sensing data from Corona declassified imagery (year 1962); 2) "reference" datasets for 2000s from Landsat ETM+ and ASTER and 3) high-resolution imagery from QB (2006) and WV (2009), all described below.

(1) Corona KH4 scenes (1962*)* were obtained from the US Geological Survey EROS Data Center (USGS-EROS, 1996). The Corona KH4 system was equipped with two panoramic cameras (forward-looking and rear-looking with 30 degrees separation angle), and acquired imagery from February 1962 to December 1963 (Dashora et al., 2007). We chose images from the end of the ablation season (October/November in this part of the Himalaya), suitable for glaciologic purposes. Six Corona stripes were scanned at 7 microns by USGS from the original film strips, with a reported nominal ground resolution of 7.62 m (Dashora et al., 2007). Corona images are known to contain significant geometric distortions due to cross-path panoramic scanning. The Frame Ephemeris Camera and Orbital Data (FECOD) camera/spacecraft parameters (roll, pitch, yaw, speed,

altitude, azimuth, sun angle and film scanning rate) for Corona missions, needed to construct a camera model and to correct these distortions, are not easily available. To orthorectify the scenes, we defined a non-metric camera model in ERDAS Leica Photogrammetric Suite (LPS), with focal length, air photo scale and flight altitude extracted from the declassified documentation of the KH4 mission (Dashora et al., 2007). We used the bundle block adjustment procedure in LPS to simultaneously estimate the orientation of all the CORONA stripes on the basis of 117 ground control points (GCPs). Latitude and Longitude (x,y) information (of the GCPs) were extracted from the panchromatic band of the 2000 Landsat ETM+ image (15 m spatial resolution) on non-glacierized terrain including moraines, river crossings, and outwash areas, whereas elevation information (z) were extracted from the SRTM DEM v.4 (CGIAR-CSI 2004). Tie points (TPs) were automatically extracted in LPS on overlapping Corona strips, and visually checked on the Landsat image. The Corona stripes were mosaicked in ERDAS LPS to produce the final orthorectified image, with a horizontal accuracy (RMSEx,y) of the bundle block adjustment of 10.5 m. The orthorectification process of the 1962 Corona yielded a RMSEx,y error of ± 10 m, and the actual "ground" RMSEx,y of the Corona block of ~60 m. A trend analysis on the horizontal shifts between Corona and the reference Landsat scene showed that the largest errors occured towards the edges of the images, mostly outside the glaciers, and did not impact the area change analysis.

(2) The orthorectified Landsat ETM+ scene from December 2000, obtained from the USGS Eros Data Center was the main dataset for the updated glacier inventory. In addition, six orthorectified ASTER products (2000 to 2002) were obtained at no cost through the Global Land Ice Monitoring from Space (GLIMS) project (Raup et al., 2007).

Images were selected at the end of the ablation season for minimal snow, and had little or no clouds. Five of these scenes were used for on-screen manual corrections of the Landsat-based glacier outlines in challenging areas where shadows or clouds obstructed the view of the glaciers. In addition, the surface kinetic temperature product (AST08) product from the November 27th, 2001 ASTER scene was used for clean ice delineation of debris cover along with topographic information using a decision-tree algorithm (Racoviteanu and Williams, 2012). The October 29th, 2002 scene, covering the Kanchenjunga-Sikkim area east and west of the topographic divide, was used to investigate the spatial distribution of surface temperature over selected debris covered tongues.

(3) Two QB scenes from January 2006 were obtained from Digital Globe as ortho-ready standard imagery (radiometrically calibrated and corrected for sensor and platform distortions) (Digital Globe, 2007). These scenes, covering an area of 1,107 km^2 were well-contrasted and mostly snow-free outside the glaciers. We orthorectified these scenes in ERDAS Imagine Leica Photogrammetry Suite (LPS) using Rational Polynomial Coefficients (RPCs) provided by Digital Globe and the SRTM DEM, and mosaicked them in ERDAS Imagine. The scenes were resampled to 3 m-pixel size during the orthorectification process using the cubic convolution method suitable for continuous raster data, in order to reduce disk space and processing time. One WorldView-2 (WV2) panchromatic, ortho-ready scene at 50 cm spatial resolution from Dec 02, 2010 was also obtained to cover the terminus of Zemu glacier, which was missing from the QB extent. All datasets were registered to UTM projection zone 45N, with elevations referenced to the WGS84 datum.

[Table 1]

Elevation datasets

Two elevation datasets were used in this study:

(1) The hydrologically-sound, void-filled CGIAR SRTM DEM (90 m spatial resolution) (CGIAR-CSI, 2004) was used to extract glacier parameters for 2000. The SRTM dataset is known to have biases on steep slopes and at higher elevations (Fujita et al., 2008; Berthier et al., 2006; Nuth and Kääb, 2011), as well as due to radar penetration on snow (Gardelle et al., 2012b). For this area, the vertical accuracy of the SRTM DEM, calculated as root mean square (RMSEz) with respect to 25 field-based GCPs, was 31 m ± 10 m. The GCPs were obtained in the field on non-glacierized terrain including roads and bare land outside the glaciers using a Trimble Geoexplorer XE series.

(2) The Swiss topographic map (1:150,000 scale), compiled from Survey of India maps from the 1960s, published by the Swiss Foundation for Alpine Research was used for manual corrections of the 1962 Corona glacier outlines to discard any seasonal snow, to correct shadow areas or bright water bodies that could be mis-classified as ice. The exact month or year of each quadrant, or of the original air photos is not known with certainty because the original large-scale Indian topographic maps at this scale are restricted within 100 km of the Indian border, and are therefore inaccessible (Srikantia, 2000; Survey of India, 2005), however this map was useful for manual corrections of the Corona outlines.

3.2 Analysis extents

We defined three analysis extents for our study area (Fig. 1 and Table 2):

(1) The Landsat/ASTER domain includes the Sikkim province of India, parts of eastern Nepal (Tamor and Arun basins), as well as parts of Bhutan and China (Table 2). This domain was used to construct the updated 2000 glacier inventory.

[Table 2]

The Landsat/ASTER domain was split into four sub-regions on the basis of east-west and north-south climate/topographic/political barriers, as shown in Fig. 3. Rainfall averages from the Tropical Rainfall Measuring Mission (TRMM) data 2B31 product (Bhatt and Nakamura, 2005; Bookhagen and Burbank, 2006) were used to characterize the sub-regions climatically. The dataset contains rainfall estimates calibrated with ground-control stations derived from local and global gauge stations (Bookhagen and Burbank, 2006) with a spatial resolution of 0.4 degree, or ~5 km. Given the well-known biases in the TRMM data (Bookhagen and Burbank, 2006; Palazzi et al., 2013; Andermann et al., 2011), here we are not concerned with the absolute values of gridded precipitation, but only with characterizing the sub-regions in our study area using relative rainfall values. TRMM data integrated over 10 years (1998 to 2007) show differences in precipitation patterns among the four regions, and justifies our choice of spatial domains (Table 3). The eastern side of the study area (Sikkim) receives higher precipitation amounts than the western side (Nepal) (977 mm/yr versus 805 mm/yr). There is a pronounced north-south gradient in precipitation, with the lowest amount of precipitation noticeable on the China side (146 mm/yr) (Table 3).

[Fig. 3 and Table 3]

(2) The Corona spatial domain is a subset of the Landsat/ASTER domain, which was covered by the 1962 Corona image. Glacier surface area changes and their dependence on

climate and topography were computed for this extent between two time steps: the 1960s decade (represented by Corona imagery), and 2000s decade (represented by Landsat/ASTER). Glaciers from Bhutan in the east and China in the north were not covered by the Corona image, so the area change analysis only focused on glaciers of Sikkim and eastern Nepal, east and west of the topographic divide.

(3) The Kanchenjunga/Sikkim domain is a smaller subset covered by all three datasets (Landsat/ASTER, Corona and Quickbird), allowing us to extend the glacier change analysis to 2006. It comprises of 50 glaciers from the Tamor basin (Nepal) and Zemu basin (Sikkim, India), located on the southern slopes of the Himalaya. The high-resolution 1962 and 2006 imagery was used here for to illustrate glacier area changes at a smaller scale, to show surface characteristics of debris-covered glaciers, and as means to evaluate mapping of debris-covered glaciers.

3.3 Glacier delineation and analysis

For the 1960s, clean glacier outlines were extracted from the panchromatic Corona imagery by thresholding the digital numbers (DN > 200 = snow/ice), chosen based on visual interpretation. Debris-covered glacier tongues were delineated manually on the basis of lateral moraines and other visual clues such as supra-glacial lakes. A 5x5 median filter was used to remove noise (isolated pixels from snowfields or internal rocks), as recommended in other studies (Racoviteanu et al., 2009; Andreassen et al., 2008). Ice polygons with area <0.02 km^2 were not considered valid glaciers and were excluded from the analysis. Manual corrections were applied subsequently on the basis of the topographic map using on-screen digitizing in areas of poor contrast or transient snow/clouds, which obstructed the view of glaciers.

For the 2000s, glaciers were delineated from the Landsat ETM+ scene using the Normalized Difference Snow Index (NDSI) (Hall et al., 1995), with a threshold of 0.7 (NDSI > 0.7 = snow/ice). The NDSI algorithm relies on the high reflectivity of snow and ice in the visible to near infrared (VNIR) wavelengths (0.4 – 1.2 μm), compared to their low reflectivity in the shortwave infrared (SWIR, 1.4 - 2.5 μm) (Dozier, 1989; Rees, 2003). Compared to other band ratios (Landsat ¾ and $^{3}/_{5}$), the NDSI glacier map was cleaner and less noisy and was therefore preferred (Racoviteanu et al., 2008b). A 5x5 median filter was used here as well to remove remaining noise, and a few areas were adjusted manually on the basis of the ASTER images, notably frozen lakes misclassified as snow/ice, and some glaciers underneath low clouds in the southern part of the image. Some transient snow persisting in the deep shadowed valleys was manually removed from the glacier outlines on the basis of the topographic map. Debris-covered glacier tongues were delineated using multispectral data (band ratios, surface kinetic temperature and texture) from the Nov 27, 2001 ASTER scene combined with topographic variables in a decision tree, as described in Racoviteanu and Williams (2012).

For the QB (2006) image, clean ice surfaces were delineated using band ratios ¾, then isodata clustering with a threshold of 1.07 (snow/ice > 1.07), and a majority filter of 7x7 to remove noise. Debris-covered tongues for this dataset were delineated manually on the basis of supraglacial features (lakes and ice walls), along with lateral and frontal moraines visible on the high-resolution images. We also mapped supraglacial lakes from this high-resolution data based on band ratios, along with texture analysis.

For all inventories in the Landsat/ASTER domain, ice masses were separated into glaciers on the basis of the SRTM DEM, using hydrologic functions in an algorithm

developed by Manley (2008), described in Racoviteanu et al. (2009). Glacier area, terminus elevation, maximum and median elevation, average slope angle and aspect were extracted on a glacier-by-glacier basis using zonal functions on the SRTM DEM. Average glacier thickness and were calculated from mass turnover principles and ice flow mechanics by Huss and Farinotti (2012), based on the approach of Farinotti (2009). Their method used our glacier outlines and the SRTM DEM to derive thickness and length estimates iteratively based on Glenn's flow law and a shape factor (Paterson, 1994). For simplicity and consistency for change analysis, we assumed no shift in the ice divides over the period of analysis, and excluded all nunataks and snow-free steep rock walls from the glacier area calculations. Bodies of ice above the bergschrund were considered part of the glacier (Racoviteanu et al., 2009; Raup and Khalsa, 2007). Glacier area changes (1962 to 2000) and their dependency on topographic and climatic variables were calculated on a glacier-by-glacier basis for the 232 glaciers in spatial domain 2 using linear regression.

3.4 Uncertainty estimates

Glacier outlines derived from remote sensing data at various spatial and temporal resolution are subject to various degrees of uncertainty, as discussed in recent studies (Paul et al., 2013; Racoviteanu et al., 2009). This becomes an important issue in glacier change analysis, where errors from various data sources accumulate at each processing step. The main sources of uncertainty considered here are: 1) image classification errors (positional errors and/or errors due to the semi-automated glacier mapping method); 2) conceptual errors associated with the definition of a glacier, including mapping of ice

1 divides, mixed pixels of snow and clouds, and internal rock differences, which propagate
2 to the glacier change analysis, all described in detail in Racoviteanu et al. (2009).
3 (1) The errors in remote sensing glacier surface areas ($E_{classif}$) were estimated using the
4 "Perkal epsilon band" around each glacier outline dataset (Racoviteanu et al., 2009;
5 Bolch et al., 2010), using a ~1-pixel variability (Congalton, 1991). Using ±30 m for
6 Landsat/ASTER, ±6 m for Corona and ±3 m for QB outlines, the area uncertainty was ±
7 3%, ±6% and ±2 % of the glacierized area for Corona, Landsat/ASTER and QuickBird
8 respectively. The Perkal method is known to slightly over-estimate the errors, as
9 described in Burrough and McDonnel (1998). Recent glacier analysis comparison
10 experiments reported a range of uncertainty of < 5% for remote sensing glacier outlines
11 compared to high-resolution imagery (Raup et al., 2007; Paul et al., 2013). For manually-
12 adjusted glacier outlines, particularly debris-covered tongues, we used screen digitizing
13 in streaming mode with a high density of vertices to minimize area errors (B. Raup,
14 National Snow and Ice Data Center, personal communication, 2014).
15 (2) Uncertainties due to different digitization of internal rocks (E_{rocks}) were derived by
16 comparing area changes computed with internal rocks specific to each dataset, versus
17 "merged" internal rocks from each dataset. The differences in glacier datasets due to rock
18 inconsistencies amounted to ~2 % of the glacier area. To minimize uncertainties in the
19 glacier area change, we merged rock outcrops from each dataset and removed them from
20 all the area calculations. The "inactive" bodies of ice above the bergschrund were
21 included as part of the glacier (Racoviteanu et al., 2009). For simplicity, we neglected the
22 area change that might be due to exposure of new internal rock due to glacier ice
23 thinning.

Total errors in glacier area estimate for each dataset (E) were calculated as RMSE of the classification ($E_{classif}$) and the internal rocks (E_{rock}):

$$E = \sqrt{E^2_{classif} + E^2_{rocks}} \qquad Eq.1$$

Errors in glacier surface area change (E_{change}) from 1962 to 2000 were computed as RMSE of the total error for each time step calculated above (Eq.1):

$$E_{1962-2000} = \sqrt{E^2_{1962} + E^2_{2000}} \qquad Eq.2$$

4. Results

4.1 The 2000 Landsat/ASTER glacier characteristics

The 2000 glacier inventory based on Landsat and ASTER yielded 487 glaciers (of which 162 were situated in Nepal, 186 in Sikkim, 30 in Bhutan and 109 in China), covering a total surface area of 1463 ± 88 km^2 (Table 4a). Of the 487 glaciers in this spatial domain, 68 glaciers (13%) had debris cover on their ablation areas. Supraglacial debris covered 160 ± 10 km^2 (11% of the glacierized area in spatial domain 1), with some differences between north and south slopes of the study area, discussed later (section 5.1). In Sikkim, supraglacial debris covered an area of 78 ± 5 km^2 in 2000 (14% of the glacierized area).

[Table 4 a-b]

In 2000, glacier size ranged from 0.02 – 105 km^2, with an average size of 3 km^2 and a median size of 0.9 km^2 (Table 4b). The histogram of glacier area (Fig. 4a) is skewed to the right (skewness = 8.4), showing that glaciers with area < 10 km^2 are predominant in this region, and glacier size decreases non-linearly. The long right-tail extremes represent only a few glaciers such as Zemu, with an area > 100 km^2.

[Fig. 4 a-d]

The average slope of all glaciers in the inventory was 23 degrees, with a positive skew (skewness = 0.38) (Fig. 4b) and no significant differences among the four regions ($p > 0.05$) (Table 4b). Glacier length ranged from 0.08 km to 23 km (Zemu glacier), with an average of 2 km (Fig. 4c). Glacier thickness ranged from 3 m to 144 m, with the highest frequency for thicknesses less than 30 m (Fig. 4d). The frequency distribution of both glacier length and thickness were positively skewed, with long tails, indicating the prevalence of short, shallow valley-type glaciers. Glacier aspect shows two predominant orientations: west-northwest (W-NW) and east-northeast (E-NE), following the topographic divide (Fig. 5). On average, glaciers on the Nepal side had an average aspect of 237 degrees (SW), whereas glaciers on the Sikkim side had an average aspect of 131 degrees (SE), consistent with local topography.

[Fig. 5]

Glacier termini elevations in the Landsat/ASTER domain ranged from 3,990 to 5,777 m, with a mean of 4,908 m; median glacier elevation ranged from 4,515 to 6,388 m, with a mean of 5,702 m (Table 4b). Considering glacier median elevation as a coarse approximation of glacier equilibrium line altitude (ELA), our results are in agreement with Benn and Owen (2005), who documented higher ELAs on the northern slopes of the Himalaya (6,000 – 6,200 m) compared to ELAs on the southern slopes (4,600 – 5,600 m).

4.2 Glacier area changes 1962 – 2000/2006

Overall, glaciers in the Corona spatial domain 2 lost 182.5 ± 40 km^2 of their area (19 ± 7% , or -0.5 ±0.2% yr^{-1}) from 1962 to 2000 (Table 5). Overall, the average glacier

area changes were slightly smaller on the western side of the divide (Nepal, 16.9± 4%1962 - 2000 or 0.44± 0.2 % yr^{-1}) compared to the eastern side (Sikkim, 20.1± 8% 1962 – 2000 or 0.52± 0.2% yr^{-1}). When focusing on a smaller glacier subset in the Kanchenjunga-Sikkim subset area (50 glaciers), we obtained an area change of -10% ± 3 % (-0.23 ±0.08% yr^{-1}) based on high-resolution imagery (1962 to 2006) (Table 5). The rates of glacier area change for this group are overall 50% lower than the rates of change in the larger spatial domain 1 perhaps due to higher percentage of debris (21 %) compared to the entire Landsat/ASTER spatial domain 2 (11%).

[Table 5]

On a glacier-by-glacier basis, glaciers in the Corona domain lost 2% to 95 % of their area, with a mean of 32% from 1962 to 2000 (Fig. 6). The spatial distribution of these area changes, illustrated in Fig. 6, shows that the largest area changes (> 70% area loss) occurred for only a few isolated glaciers in the northern and southern extremities of the study area (17 glaciers). A closer examination of these glaciers revealed that these were small clean glaciers (< 0.1 km^2), with steep slopes (mean of 26 degrees), posing a need to investigate the topographic controls on area change, and clean vs. debris-covered glaciers separately.

[Fig. 6]

Clean glaciers lost more of their area from 1962 to 2000 (34%) compared to debris-covered glaciers (22 %) across the region, with little differences east-west (Nepal and Sikkim)(Table 6). The difference in mean rates of area change between clean and debris covered glaciers was statistically significant based on two-sample F-test (p-value < 0.05).

[Table 6]

Fig. 7a-b, shows a larger spread and a higher percentage of surface area loss of clean glaciers compared to debris-covered glaciers. For both glacier types, however, there is a high variability in percent area change, perhaps due to other factors such as local topography.

[Fig. 7 a-b]

Linear regression analysis showed that percent area change per glacier was negatively correlated to glacier area, altitudinal range, glacier elevation (median and maximum elevation and aspect (significant correlations at 99% confidence interval, $p<0.01$) (Table 7). Glacier minimum elevation and slope were significant controls on glacier area change at 95% confidence interval ($p < 0.05$). Solar radiation, precipitation and percent debris were not statistically significant controls on glacier area change ($p>0.1$, confidence interval 90%) (Table 7). These are discussed in section 5.3.

[Table 7]

Clean and debris-covered glaciers showed significant differences in terms of glacier area, area change, minimum elevation, altitudinal range and length based on a two sample F-test for variances) ($p < 0.05$) (Table 8). Clean glaciers in this area are ~12 times smaller (1 km^2 on average) than debris-covered glaciers (15 km^2), they have higher termini elevations (+ 391 m), and an overall altitudinal range about 3 times smaller than debris-covered glaciers (Table 7). On a glacier-by-glacier basis, clean glaciers lost more area (34 %) than debris covered glaciers (22%) from 1962 to 2000. Clean glaciers with smaller altitudinal range tend to display more area loss compared to debris-covered glaciers.

[Table 8]

5. *Discussion*

5.1 Spatial distribution of glacier characteristics across the study area

One of the important steps in utilizing our glacier inventory data is to understand spatial patterns in glacier characteristics across the region. Our study area displays region-wide consistency in glacier characteristics notably glacier area, elevation and topography across four sub-regions based on the 2000 glacier data (Table 4). For example, the prevalence of small glaciers noted in this area is consistent with worldwide patterns, also observed for the Cordillera Blanca of Peru in a previous study (Racoviteanu et al, 2008a). There is variability within eastern Himalaya, for example the mean glacier size reported in this study area (3 km^2) is double compared to Khumbu region, west of our study area (1.4 km^2) (Bajracharya and Shrestha, 2011). The glacier slope across our study area (23 degrees) is consistent with average glacier slopes reported for the Khumbu region in Nepal (22 degrees) (Bajracharya and Shrestha, 2011; Salerno et al., 2008), indicating a general tendency for steep glaciers across the region. There are only a few large, long glaciers in the area such as Zemu glacier (103 km^2, 23 km in 2000). With respect to glacier aspect, we also note similar predominant orientations of glaciers southwards, in the direction of the prevailing monsoon circulation consistent with other studies such as the Khumbu region (average aspect 181 degrees) (Mool et al., 2002; Salerno et al., 2008).

The comparison of glacier characteristics across sub-regions points to a pronounced gradient north to south (Bhutan/China sub-regions compared to Sikkim/Nepal), particularly with respect to glacier elevations and debris cover. Glaciers on northern side of the divide (China) have higher glacier termini and median elevations compared to the

southern side (Nepal and Sikkim) (+700 m and +400 m respectively) (Table 4). These differences seem to be consistent with general air circulation patterns in the area. The Asian summer monsoon brings large amounts of precipitation on the southern slopes of the Himalaya, favoring glacier growth at lower elevations and a lower ELA. In contrast, in the upper reaches of the valleys and on the Tibetan plateau, the monsoon is blocked by the topographic barrier (Clift and Plumb, 2008), causing a drier climate and higher glacier ELAs. There is a much less pronounced east-west gradient in glacier elevations, with higher glacier minimum and median elevations on the western side (Nepal) (+50 m) compared to the eastern side (Sikkim). This may be explained by the location of Nepalese glaciers on the western side of the topographic divide, away from the prevailing monsoon.

Debris coverage also shows a pronounced variability north to south of the topographic divide. Himalayan glaciers are often referred to as "heavily" debris-covered, but the percent glacierized area covered by supra-glacial debris cover varies across the mountain range. In our study area, debris cover is more prevalent on the southern side of the divide (Sikkim, 14% of glacierized area) compared to the northern one (China, 2% of the glacierized area), perhaps due to different geologic and topographic patterns. The northern side of the divide, which is part of the Tibetan plateau, is situated in a monsoon shadow and is therefore dry; the gentler slopes induce lower rates of erosion. In contrast, the southern slopes of the Himalaya tend to be heavily covered with debris cover due to the abundance of rock material from the steep slopes. The steep slopes made of soft sedimentary rocks and Precambrian crystalline rocks (Mool et al., 2002) and are prone to high rates of erosion, particularly with large amounts of monsoon moisture. This north-

1 south difference in debris cover amount was also noted in other studies (Scherler et al.,
2 2011). In our study, we found a lower percent of debris coverage (21%) than the entire
3 central/eastern Himalaya reported in Scherler et al. (2011) (36% debris cover), or from
4 the Khumbu region, west of our study area, by Fujii and Higuchi (1977), Nuimura et al.
5 (2012) (34.8%), Racoviteanu et al. (2013a) (27 %) and Thakuri et al. (2014) (32%).

6 *5.2 Regional glacier area changes*

7 The overall rate of surface area loss of 0.5 ± 0.2% yr^{-1} from 1962 to 2000 for Sikkim
8 and eastern Nepal obtained here is in agreement with other studies from the southern
9 slopes of the Himalaya. Similar rates of area loss (0.1 to 0.3% yr^{-1}) were reported from
10 the Khumbu and Garwhal regions, west of our study area, for approximately the same
11 time period (Thakuri et al., 2014; Basnett et al., 2013; Nuimura et al., 2012; Bolch et al.,
12 2008a; Bhambri et al., 2011). Similarly, for glaciers of Bhutan, east of our study area,
13 Karma et al. (2003) found an average surface glacier area loss of 0.3% yr^{-1} from 1963 to
14 1993. It is worth mentioning that these rates of area change are lower than those
15 previously reported for the drier monsoon-transition zone in the western Himalaya (0.7%
16 yr^{-1}) by Kulkarni et al. (2007), which raised concerns about the future of Himalayan
17 glaciers. In a more recent study, Bahuguna et al. (2014) found lower rates of glacier area
18 loss (0.4% yr^{-1}) for the same area (Himachal Pradesh in the western Himalaya), which is
19 in agreement with rates of area loss we report here for eastern part. Updated glacier area
20 changes from recent studies (Bahuguna et al., 2014; Racoviteanu et al., 2014; Bolch et
21 al., 2012) also point at lower rates of area loss than previously reported, particularly for
22 the Indian Himalaya. The similar overall rate of glacier area change in the eastern part

compared to western one for both debris covered glaciers and clean glacier types suggest consistent patterns across the region (Table 5).

The smaller glacier area loss for debris-covered glaciers noted in our study is in agreement with studies from Khumbu (Nuimura et al., 2012; Thakuri et al., 2014) or other studies in the central-eastern Himalaya (Bolch et al., 2008a; Thakuri et al., 2014; Bhambri et al., 2011). These studies also reported lower rates of glacier surface area loss and even stable or less retreating glacier termini for debris-covered tongues compared to clean glaciers (Scherler et al., 2011). Area changes for debris-covered glaciers need to be interpreted with caution, due to the wide variability in debris cover characteristics such as thickness. Furthermore, these stagnating or less changing tongues may not reflect the true state of the glaciers, for example patterns of glacier thinning, which may occur at similar rates to clean glaciers (Gardelle et al., 2012a; Kääb et al., 2012).

5.3 Topographic and climatic controls on area changes

While the consistent area change patterns across the sub-regions (east to west) are useful for comparison with larger areas, these patterns cannot be used to understand glacier-by-glacier variability in area changes, which may be controlled by local topography and climate. In this study, we found that topographic factors, notably glacier size, glacier altitude (maximum, median, altitudinal range) and aspect were most important in determining rates of glacier area loss in spatial domain 1. Glacier size plays a significant role in determining area change, i.e. smaller glaciers experienced higher rates of area loss (Table 7). The tendency of larger glaciers to lose less area (>20 km^2) was observed in various studies (Racoviteanu et al., 2008a; Salerno et al., 2008; Loibl et al., 2014), though in the case of Salerno et al. (2008), for the Khumbu, the correlation

was not statistically significant. Higher glacier elevations and larger altitudinal ranges significantly reduce the rates of area loss, as was also noted in the Khumbu region in Nepal and elsewhere. The dependency of area change on glacier size and elevation is also consistent with observations from the Cordillera Blanca of Peru (Racoviteanu et al., 2008a) in the outer tropics, indicating consistent patterns in glacier area changes worldwide.

[Table 7]

Glacier slope also plays a significant role in determining glacier area change, i.e. the steeper the glacier, the larger the area loss observed in our study. The same tendency was observed in the Khumbu area (Salerno et al., 2008), but the correlation is less significant than the glacier altitude ($p<0.05$). The presence of gentle slopes covered with supra-glacial debris in the ablation areas of glaciers, fairly common in this area, may have reduced the strength of the correlation. Glacier aspect was also found to be a significant control on area change, with more area loss for glaciers oriented southwards and south-west ($p<0.01$). This is in agreement with findings from Salerno et al. (2008) for the Khumbu region, but is in contrast with results from Loibl et al. (2014) for the Nyainqêntanglha Range in southeastern Tibet, about 600 km east of our study area, who found that south-facing glaciers experienced smaller rates of terminus retreat. Percent debris cover was a negative control on area change, i.e. glaciers with more extensive debris cover on their areas tend to lose less area overall, but this was not statistically significant ($p >0.05$). Debris covered glaciers may benefit from the insulating effect of debris cover above a certain "critical" debris thickness (Mihalcea et al., 2008a; Zhang et al., 2011), which needs to be further investigated.

Geographic location (latitude and longitude) were negative controls on glacier area change suggesting that glaciers located north and eastwards of the study area tend to lose more area, but only latitude was statistically significant ($p < 0.05$). Climate indices (precipitation and solar radiation) were not significant factors controlling glacier area loss. In contrast, Loibl et al. (2014) showed that glaciers located in a monsoon-influenced area were more sensitive to climate change. This is in agreement with larger-scale studies (Gardelle et al., 2013), which indicated a tendency for enhanced glacier wastage in the eastern, monsoon-influenced parts of the Himalaya. With respect to climatic factors in this area, Basnett et al. (2013) reported an increase in mean annual temperature, more significantly in the winter (+2°C yr^{-1} in the last four decades). Increasing temperatures on the south slopes of the Himalayas were also noted in other studies (Shrestha et al., 2000; Thakuri et al., 2014) based on instrumental data, but were estimated to have less effect on glacier area than changes in precipitation because of the orientation of these glaciers towards the prevailing monsoon circulation. In our study, the climatic control on glacier area is not conclusive, and finer-resolution, more accurate temperature and precipitation datasets would be needed. Furthermore, similarly to areas further east (Loibl et al., 2014), average annual solar radiation and latitude were not found to be significant controls on glacier area change in our study.

5.4 Surface temperature distribution on debris cover tongues

Smaller rates of area change for the debris-covered glaciers may be further explained by surface characteristics of debris cover (thickness, thermal conductivity and resistance). However, these are not easily available in this area due to the lack of field-based measurements, and the difficulty of conducting surveys on the debris-covered tongues.

Therefore, in this study, we are qualitatively showing the distribution of surface temperature on selected debris-covered tongues in spatial domain 3 based on the 2002 ASTER scene. Fig. 8 shows a high variability in supra-glacial surface temperature at 90 m spatial resolution, but there is no clear general temperature trend for the eastern slopes (Sikkim side) versus the western slopes (Nepal) side. The fluctuations in surface temperatures along transects are clearly visible on Fig. 9, with some sharp spikes of high and low temperatures, particularly for Kanchenjunga and Yalung glaciers (labeled "A" and "B" on Fig. 8). This strong variability in supraglacier debris temperatures may be due to the presence of surface features such as debris thickness, size of the debris particles, and thermal resistance and conductivity of the debris. For the debris-covered tongues investigated here, the supraglacier temperatures range from 0ºC to 30ºC, suggesting that the supra-glacier debris heats up considerably during the day. At the glacier scale, temperature drops over supraglacial features such as ice walls and supra-glacial lakes, which tend to be colder than the surrounding debris, and this is visible even at the coarse spatial resolution of the temperature data (90 m). On Fig. 9 we note the slight upward trend for supra-glacier temperature towards the glacier termini, particularly for Zemu glacier ("C" on Fig. 8). For this glacier, the middle-upper part of the debris surface is colder (-3 to 5ºC) than the last 10 km towards the glacier terminus (5 to 14ºC) (Fig. 9). In a different paper (Racoviteanu and Williams, 2012), we found similar patterns of surface temperature increasing towards the glacier terminus for the same glacier, but based on a different scene (November 2001), indicating consistent patterns for this glacier. The higher surface temperatures towards the glacier terminus may indicate a thicker debris cover, which insulates the ice underneath, noted on other studies (Mihalcea et al., 2008a).

The daytime debris temperature ranges and the strong spatial variability noted here are similar to the ones we found for Khumbu, west of this study area (-3 to 17ºC) (Racoviteanu et al., 2013b). In Khumbu, we found that supra-glacier debris had a distinct temperature signal compared to other surfaces such as non-ice moraine, clean ice, and supra-glacier/pro-glacier lakes, with more pronounced differences among these three during the daytime.

[Fig. 8 and 9]

The suitability of ASTER-based surface for inferring debris characteristics, most notably thickness, has been demonstrated in other studies (Mihalcea et al., 2008a; Zhang et al., 2011). For this study area, there were no field measurements available to test the validity of ASTER temperatures for quantifying supra-glacier debris characteristics. However, in a different study (Racoviteanu et al., 2013b), we validated ASTER-based surface temperatures extracted from 9 night scenes from 2010 – 2011 for the Khumbu by inverting field-based long-wave radiation (L_{out}) using the Stefan-Bolzmann law ($L_{out} = \varepsilon T^4$). The measurements were from the automatic weather station (AWS) installed on Changri Nup glacier (Wagnon et al., 2013). We found a good agreement between ASTER temperatures and field-based measurements ($R^2 = 0.92$) using a sensitivity analysis ($\varepsilon = 0.97 \pm 0.1$) to account for small-scale variability in emissivity. Given that the Kanchenjunga-Sikkim area has similar characteristics to Khumbu in terms of debris cover, geographic location, and that the images were acquired around the same time of the year as the Khumbu (Nov.- Jan.), we consider that this validation may be applicable to the present study area.

5.4 The role of glacier lakes

The role of supra-glacier/pro-glacier lakes for glacier area change in this area of the Himalaya was addressed in detail in recent studies (Basnett et al., 2013; Bajracharya et al., 2014). Gardelle et al. (2011) also pointed out the increased formation of supra-glacier lakes particularly for the eastern part of the Himalaya. A quantitative assessment of lake formation is beyond the scope of this paper; here we only illustrate qualitatively some of the changes occurring on glaciers with supra-glacial or pro-glacial lakes using high-resolution Corona and QuickBird imagery. For the Tista basin in Sikkim, Mool and Bajracharya (2003) inventoried 266 glacier lakes covering a total area of 20 km^2 (3.5% of the glacierized area) based on 2000 Landsat ETM+ imagery. For spatial domain 3, we estimated that glacier lakes covered 1.3% of the total debris-covered glacier area, or 5.8% of the area if we consider only the debris-cover (ablation) part, based on the QB/WV2 imagery. Salerno et al. (2012) reported similar percentage for the area of supraglacial lakes, i.e. (0.3 – 2% of the overall glacierized area) for the Khumbu region. While supra-glacier lakes do not cover extensive areas of the glacierized surface, they were shown to increase surface ablation rates in this part of the Himalaya (Fujita and Sakai, 2014; Sakai et al., 2002). It was also shown that supra-glacier lakes located at the glacier terminus tend to merge to create large, fast growing pro-glacier lakes which accelerate glacier area loss (Basnett et al., 2013; Bajracharya et al., 2014).

Some of the pro-glacier lakes in our study area are visible on Fig. 10 and 11 for the northern part of spatial domain 3 (Changsang, East Langpo, Jongsang, Middle Lhonak, South Lhonak). Most of these lakes are moraine-dammed lakes, considered dangerous for potentially inducing glacier lake outburst flood events, and were shown to accelerate the

glacier area loss in the recent decades (Bajracharya et al., 2014). Fig.10 a-b shows the evolution of the pro-glacier lake on N. and S. Lhonak glaciers in Sikkim, also noted in Basnett et al. (2013). A closer look at a subset area (Fig. 11) shows the visible growth of a pro-glacial lake for the adjacent N. Lhonak and S. Lhonak glaciers. We estimate that these two glaciers retreated ~650 m and 1.3 km from 1962 to 2006, respectively. Another branch of N. Lhonak glacier has wasted significantly by ~1.5 km from 1962 to 2006, and a glacier outlet is now clearly visible. The northern branch of Jongsang glacier was entirely covered by a supra-glacier lake in 2006, while another part shows less significant rates of terminus retreat (~100 m in 44 years). A part of the Jongsang glacier shows a slight "false" glacier tongue advance, most likely due to uncertainties in the mapping of Corona imagery. While our purpose here is not to present glacier length changes, we note that these estimates are in agreement with trends of glacier thinning and increased glacier lake formation reported in this area of the Himalaya previously (Gardelle et al., 2011; Basnett et al., 2013; Kääb et al., 2012).

[Fig. 10 and 11]

5.5 Uncertainty and limitations

Inconsistencies in glacier area change estimates have been pointed out in other studies, for the Himalaya and elsewhere (Racoviteanu et al., 2008b; Racoviteanu et al., 2008a), and are also noted in the current study. Glacier area changes in the Himalaya are heterogeneous, and depend on a variety of factors including local topography and climate, so some caution should be applied when comparing rates of area changes from one area to other areas, even in the same climatic zone. For example, for Sikkim, we estimated a surface area change of -88.9 ± 5 km^2 (-13.5% from 1962 to 2006, or -0.36 ±

1 0.17 % yr^{-1}). Other studies in this area point to contrasting results. For the same
2 geographic area, Basnett et al. (2013) reported an area change of -0.16 ± 0.10 % yr^{-1} from
3 1989/1990 to 2009/2010), which about half of the area change in our findings. In
4 contrast, a recent study (Bahuguna et al., 2014) reported the highest rates of area change
5 (about -0.8% yr^{-1}) for the last decade, even higher than rates reported previously for the
6 western Himalaya by Kulkarni et al. (2007). We speculate that such large differences
7 might be due to errors inherent in the baseline datasets, coupled with misclassification
8 due to snow cover or debris-covered areas.

9 Glacier area changes reported for Sikkim in different studies, using a variety of
10 data, including topographic maps (Table 9), illustrates this point. For example, for
11 Sikkim, our study estimated 569 km^2 ± 70 km^2 of glacierized area in 2000 based on
12 Landsat/ASTER data. For the same time period, Mool et al. (2002) reported an area of
13 577 km^2 based on the same source imagery (Landsat ETM+) (Table 9). These two area
14 estimates differ only by 8.2 km^2 (1.4%) of our estimated area, only the number of glacier
15 differs substantially (186 glaciers in our study compared to 285 glaciers in ICIMOD
16 study), most likely due to the way in which ice masses were split and how glaciers were
17 counted. Methodology differences and inconsistencies in glacier estimates are quite
18 common in multi-temporal image analysis performed by different analysts, and were
19 previously noted in other areas of the world (Racoviteanu et al., 2009). Similarly, for the
20 1962 decade, our analysis of Corona 1962 imagery for Sikkim yielded 178 glaciers with
21 an area of 658 ± 20 km^2. In a recent publication (Racoviteanu et al., 2014), we reported
22 158 glaciers with an area of 742 km^2 for the 1960s based on the Swiss topographic map.
23 The Geological Survey of India (GSI) (Sangewar and Shukla, 2009) reported 449 glaciers

with an area of 706 km^2 for the 1970s based on topographic maps. Our 1962 Corona glacier inventory yields a smaller total glacier area than the one based on the topographic map (84 km^2, or 11%) (Racoviteanu et al., 2014) or the GSI inventory based on topographic maps (48.3 km^2, or 7 % area) (Sangewar and Shukla, 2009). We consider that both of these mentioned studies overestimated the glacier area in the 1960s, perhaps due to the presence of persistent snow in the source aerial imagery.

Subsequent glacier inventories in Sikkim also point to contradictory patterns. For the 1980s, another study (Kulkarni, 1992b) reported a glacierized area of 431 km^2 for 1987/1989 based on Indian IRS-1A and Landsat data. Considering our 1962 Corona inventory, this would imply an area loss of 42% since 1962 (2.1% yr^{-1}), followed by a strong increase in glacier area (+33.5 %, or +3% yr^{-1}) from 1987/1988 to 2000 (based on our Landsat analysis), which is undocumented in this area. We consider the 1987/89 estimates to be highly unreliable, given that there are no glacier surges that might induce an apparent "glacier growth". In some areas, we noted omissions of some debris-covered tongues from the glacier maps, which might explain some of the differences. We consider the Corona 1962 dataset to be more reliable than the inventories based on topographic maps, and hence we used this dataset as baseline for comparison with the recent imagery.

[Table 9]

6. Summary and outlook

In this study we combined remote sensing data from various sensors to construct a new glacier inventory for the Kanchenjunga-Sikkim region in the eastern Himalaya. Based on 1962 Corona and 2006 QuickBird imagery, we found an overall negative

glacier surface area change of 0.5±0.2% yr^{-1} since 1962, in agreement with those noted in other studies in the Himalaya. The area change rates reported here are lower than the average rate of -0.7% yr^{-1} reported in other glacierized areas of the world such as the Alps (Kääb et al., 2002), the Tien Shan (Bolch, 2007) and the Peruvian Andes (Racoviteanu et al., 2008a). Glaciers exhibit heterogeneous patterns of area change, depending on topographic and climatic factors, more notably glacier altitude (maximum, median, altitudinal range), glacier size, slope and aspect. Glacier area changes depend strongly on glacier size and elevation, which is consistent with other areas in the central-eastern Himalaya (Thakuri et al., 2014) or elsewhere, for example the outer tropics (Racoviteanu et al., 2008a). The conclusions drawn with respect to spatial patterns in glacier characteristics, glacier area loss, and their topographic and climatic dependency, include:

- We found a strong north-south gradient in terms of glacier elevations and debris cover, with larger percent of area covered by debris, and higher glacier elevations on the northern side for the divide, but less east to west gradient in these characteristics;
- Glacier area change (loss) of 0.5 % ± 0.2% yr^{-1} from 1962 to 2000, with some differences on the eastern side of the divide (Sikkim, -0.52 % ± 0.2% yr^{-1}) versus the western part (Nepal, -0.44 % ± 0.2% yr^{-1});
- Higher rates of area loss for clean glaciers (-34 %, or -0.7% yr^{-1}) compared to debris-covered glaciers (-14.3% or -0.3 yr^{-1}) across the sub-regions on a glacier-by-glacier basis;
- The amount of glacier area loss is partly controlled by a glacier's headwater elevation, altitudinal range, glacier area, slope and aspect, with the largest area

loss observed for small, steep glaciers with a smaller altitudinal range and less debris cover;

- Supraglacial debris cover is prevalent on the southern slopes of the Himalaya (14% of the glacierized area) compared to northern slopes (2%);
- Supraglacial lakes constitute about 6% of the debris covered area, and some of these supra-glacial lakes have merged to form pro-glacial lakes;
- While Himalayan glaciers are undoubtedly undergoing negative area change, the rates of area loss noted in this study (0.5% yr^{-1}) as well as other recent studies in the area (0.2 – 0.4% yr^{-1} since the 1960s) are lower than other glacierized areas worldwide (0.7% yr^{-1}).

The glacier area change estimates reported here are subject to uncertainties, most notably with respect to early topographic maps and declassified Corona imagery, therefore a considerable effort was given to minimizing errors by multiple re-iterations of the glacier outlines. The understanding of the spatial patterns of glacier changes in the current study is limited by: 1) a lack of a baseline elevation dataset for the 1960 to compute glacier elevation changes from 1960s to 2000; 2) lack of field-based measurements to validate debris-cover mapping and surface temperature distribution. With respect to the latter, while surface temperature trends show a slight increase towards the terminus, suggesting a thicker debris cover, the supra-glacial surface temperatures are highly heterogonous and require additional investigation. A further improvement in the current study will be to include the supra-glacial and pro-glacial lakes and surface temperature as determinant factors for the glacier area change, perhaps in a more sophisticated multivariate regression model. The glacier datasets constructed in this study

can be further utilized to understand the behavior of glaciers in this little-investigated area of the Himalaya, particularly with respect to spatial patterns of glacier melt, and the contribution of glaciers to water resources.

Acknowledgements

This research was funded by a NASA Earth System Sciences (ESS) fellowship (NNX06AF66H), a National Science Foundation doctoral dissertation improvement grant (NSF DDRI award BC 0728075), a CIRES research fellowship, a graduate fellowship from CU-Boulder and a post-doc fellowship from Centre National d'Etudes Spatiales (CNES), France. Participation of M. Williams was supported by the NSF-funded Niwot Ridge Long-Term Ecological Research (LTER) program and the USAID Cooperative Agreement AID-OAA-A-11–00045. ASTER imagery was obtained through the NASA-funded Global Land Ice Measurements from Space (GLIMS) project. We are grateful to Jonathan Taylor at University of California-Fullerton for facilitating access to high-resolution imagery through the NASA Appropriations Grant # NNA07CN68G. We thank Dr. Damodar Lamsal and an anonymous reviewer for their thorough comments, which helped improve the quality of the manuscript.

References

Ageta, Y., and Higuchi, K.: Estimation of Mass Balance Components of a Summer-Accumulation Type Glacier in the Nepal Himalaya, Geografiska Annaler Series A-Physical Geography, 66, 249-255, 1984.

Andermann, C., Bonnet, S., and Gloaguen, R.: Evaluation of precipitation data sets along the Himalayan front, Geochemistry, Geophysics, Geosystems, 12, Q07023, 10.1029/2011gc003513, 2011.

1 Andreassen, L. M., F. Paul, A. Kääb, and J. E. Hausberg: The new Landsat-derived
2 glacier inventory for Jotunheimen, Norway, and deduced glacier changes since the
3 1930s, Cryosphere Discuss, 2, 299-339, 2008.

4 Bahuguna, I. M., B. P. Rathore1, Brahmbhatt, R., Sharma, M., Dhar, S., Randhawa, S. S.,
5 Kumar, K., Romshoo, S., Shah, R. D., and Ganjoo, R. K.: Are the Himalayan glaciers
6 retreating?, Curr Sci, 106, 1008-1013, 2014.

7 Bajracharya, S. R., Mool, P. K., and Shresta, A.: Impact of climate change on Himalayan
8 glaciers and glacial lakes, ICIMOD, Kathmandu, 2007.

9 Bajracharya, S. R., Maharjan, S. B., and Shresta, F.: The status and decadal change of
10 glaciers in Bhutan from 1980's to 2010 based on the satellite data, Annals of
11 Glaciology, 55, 159-166, doi: 10.3189/2014AoG66A125, 2014, 2014.

12 Basnett, S., Kulkarni, A., and Bolch, T.: The influence of debris cover and glacial lakes
13 on the recession of glaciers in Sikkim Himalaya, India, Journal of Glaciology, 59,
14 1035 - 1046, 2013.

15 Benn, D., and Owen, L. A.: Equilibrium-line altitudes of the Last Glacial Maximum for
16 the Himalaya and Tibet: an assessment and evaluation of results, Quaternary Int, 138 -
17 139, 55 -58, 2005.

18 Benn, D. I., and Owen, L. A.: The role of the Indian summer monsoon and the mid-
19 latitude westerlies in Himalayan glaciation: review and speculative discussion, Journal
20 of the Geological Society, 155, 353-363, 1998.

21 Berthier, E., Arnaud, Y., Vincent, C., and Remy, F.: Biases of SRTM in high-mountain
22 areas: Implications for the monitoring of glacier volume changes, Geoph Res Lett, 33,
23 L08502. doi:08510.01029/ 02006GL025862, 2006.

24 Berthier, E., Arnaud, Y., Kumar, R., Ahmad, S., Wagnon, P., and Chevallier, P.: Remote
25 sensing estimates of glacier mass balances in the Himachal Pradesh (Western
26 Himalaya, India), Remote Sensing of Environment, 108, 327 - 338, 2007.

27 Bhambri, R., and Bolch, T.: Glacier mapping: a review with special reference to the
28 Indian Himalayas, Progr Phys Geogr, 33, 672-702, 2009.

29 Bhambri, R., Bolch, T., Chaujar, R. K., and Kulshreshth, S. C.: Glacier changes in the
30 Garhwal Himalayas, India during the last 40 years based on remote sensing data.,
31 Journal of Glaciology, 54, 543-556, 2010.

32 Bhambri, R., Bolch, T., Chaujar, R. K., and Kulshreshtha, S. C.: Glacier changes in the
33 Garhwal Himalaya, India, from 1968 to 2006 based on remote sensing, Journal of
34 Glaciology, 57, 543-556, 2011.

1 Bhatt, B. C., and Nakamura, K.: Charactieristics of Monsoon rainfall around the
2 Himalayas revealed by TRMM precipitation radar, Monthly Weather Review, 133,
3 149-165, http://dx.doi.org/10.1175/MWR-2846.1, 2005.

4 Bolch, T.: Climate change and glacier retreat in northern Tien Shan
5 (Kazakhstan/Kyrgyzstan) using remote sensing data, Global Planet Change, 56, 1-12,
6 2007.

7 Bolch, T., Buchroithner, M. F., Pieczonka, T., and Kunert, A.: Planimetric and
8 Volumetric Glacier Changes in the Khumbu Himalaya since 1962 Using Corona,
9 Landsat TM and ASTER Data, J Glaciol, 54, 592-600, 2008a.

10 Bolch, T., M.F.Buchroithner, J.Peters, M.Baessler, and Bajracharya, S.: Identification of
11 glacier motion and potentially dangerous glacial lakes in the Mt. Everest region/Nepal
12 using spaceborne imagery, Nat.Hazards Earth Syst. Sci, 8, 1329-1340, 2008b.

13 Bolch, T., Menounos, B., and Wheate, R.: Landsat-based inventory of glaciers in western
14 Canada, 1985–2005, Remote Sensing of Environment, 114, 127-137, 2010.

15 Bolch, T., Pieczonka, T., and Benn, D. I.: Multi-decadal mass loss of glaciers in the
16 Everest area (Nepal Himalaya) derived from stereo imagery, The Cryosphere, 5, 349-
17 358, 10.5194/tc-5-349-2011, 2011.

18 Bolch, T., Kulkarni, A., Kääb, A., Huggel, C., Paul, F., Cogley, J. G., Frey, H., Kargel, J.
19 S., Fujita, K., Scheel, M., Bajracharya, S., and Stoffel, M.: The State and Fate of
20 Himalayan Glaciers, Science, 336, 310-314, 10.1126/science.1215828, 2012.

21 Bookhagen, B., and Burbank, D. W.: Topography, relief and TRMM-derived rainfall
22 variations along the Himalaya, Geoph Res Lett, 33, doi::10.1029/2006gl026037, 2006.

23 Burrough, P. A., and McDonnel, R. A.: Principles of Geographic Information Systems.,
24 Oxford University Press, 1998.

25 CGIAR-CSI. Void-filled seamless SRTM data V1: http://srtm.csi.cgiar.org;
26 http://www.ambiotek.com/topoview, access: 2014-04-01, 2004.

27 Clift, P. D., and Plumb, R. A.: The Asian Monsoon: Causes, History and Effects,
28 Cambridge University Press, New York, 88 pp., 2008.

29 Congalton, R. G.: A review of assessing the accuracy of classifications of remotely
30 sensed data, Rem Sens Environ, 37, 35-46, 1991.

31 Dashora, A., Lohani, B., and Malik, J. N.: A repository of Earth resource information-
32 CORONA satellite programme, Current Science, 92, 926-932, 2007.

33 QuickBird Imagery Products- Product Guide. Revision 4.7.3:
34 http://www.hatfieldgroup.com/UserFiles/File/GISRemoteSensing/ResellerInfo/Quick
35 Bird/QuickBird Imagery Products - Product Guide.pdf, access: 08-15, 2007.

1 Dozier, J.: Spectral Signature of Alpine Snow Cover from the Landsat Thematic Mapper,
2 Remote Sensing of Environment, 28, 9-22, 1989.

3 Farinotti, D., Huss, M., Bauder, A., and Funk, M.: An estimate of the glacier ice volume
4 in the Swiss Alps, Global and Planetary Change, 68, 225-231, 2009.

5 Foster, L. A., Brock, B. W., Cutler, M. E. J., and Diotri, F.: A physically based method
6 for estimating supraglacial debris thickness from thermal band remote-sensing data,
7 Journal of Glaciology, 58, 677-690, 2012.

8 Frey, H., Paul, F., and Strozzi, T.: Compilation of a glacier inventory for the western
9 Himalayas from satellite data: methods, challenges, and results, Remote Sensing of
10 Environment, 124, 832-843, http://dx.doi.org/10.1016/j.rse.2012.06.020, 2012.

11 Fujii, Y., and Higuchi, K.: Statistical analyses of the forms of the glaciers in Khumbu
12 Himal, Seppyo, 39, 7-14, 1977.

13 Fujita, K., Suzuki, R., Nuimura, T., and Sakai, A.: Performance of ASTER and SRTM
14 DEMs, and their potential for assessing glacial lakes in the Lunana region, Bhutan
15 Himalaya, J Glaciol, 54, 220-228, 2008.

16 Fujita, K., and Sakai, A.: Modelling runoff from a Himalayan debris-covered glacier,
17 Hydrol Earth Syst Sci Discuss, 11, 2441-2482, 2014.

18 Gardelle, J., Arnaud, Y., and Berthier, E.: Contrasted evolution of glacial lakes along the
19 Hindu Kush Himalaya mountain range between 1990 and 2009, Global and Planetary
20 Change, 75, 47-55, 10.1016/j.gloplacha.2010.10.003, 2011.

21 Gardelle, J., Berthier, E., and Arnaud, Y.: Slight mass gain of Karakoram glaciers in the
22 early twenty-first century, Nature Geoscience, Nature Geoscience, 5, 322-325, 2012a.

23 Gardelle, J., Berthier, E., Arnaud, Y., and Kaab, A.: Region-wide glacier mass balances
24 over the Pamir-Karakoram-Himalaya during 1999 - 2011, The Cryosphere, 7, 1263 -
25 1286, doi:1210.5194/tc-1267-1263-2013, 2013.

26 Gardelle, J. E., Berthier, E., and Arnaud, Y.: Impact of resolution and radar penetration
27 on glacier elevation changed computed from DEM differencing, Journal of
28 Glaciology, 58, 419-422, 2012b.

29 Hall, D. K., G. Riggs, A., and Salomonson, V. V.: Development of methods for mapping
30 global snow cover using moderate resolution imaging spectroradiometer data, Rem
31 Sens Environ, 54, 127-140, 1995.

32 Huss, M., and Farinotti, D.: Distributed ice thickness and volume of all glaciers around
33 the globe, Journal of Geophysical Research, 117, DOI: 10.1029/2012JF002523, 2012.

34 IMD: Climatological tables 1951 - 1980, Government of India, Controller of Publication,
35 New Delhi, 1980.

1 Immerzeel, W., van Beek, L. P. H., and Bierkens, M. F. P.: Climate Change Will Affect
2 the Asian Water Towers, Science, 328, 1382-1385, 10.1126/science.1183188, 2010.

3 Immerzeel, W. W., Beek, L. P. H. v., Konz, M., Shrestha, A. B., and Bierkens, M. F. P.:
4 Hydrological response to climate change in a glacierized catchment in the Himalayas,
5 Climatic Change, 110, 721-736, 2012.

6 Iwata, S., Aoki, T., Kadota, T., Seko, K., and Yamaguchi, S.: Morphological evolution of
7 the debris cover on Khumbu Glacier, Nepal, between 1978 and 1995, in: Debris-
8 covered glaciers, edited by: Nakawo, M., Raymond, C. F., and Fountain, A., IAHS, 3 -
9 11, 2000.

10 Kääb, A., Paul, F., Maisch, M., Hoelzle, M., and Haeberli, W.: The new remote-sensing-
11 derived Swiss glacier inventory: II. First results, Annals of Glaciology, 34, 362-366,
12 2002.

13 Kääb, A., Berthier, E., Nuth, C., Gardelle, J., and Arnaud, Y.: Contrasting patterns of
14 early twenty-first-century glacier mass change in the Himalayas, Nature, 488, 495-
15 498, http://www.nature.com/nature/journal/v488/n7412/abs/nature11324.html -
16 supplementary-information, 2012.

17 Kamp, U., Byrne, M., and Bolch, T.: Glacier fluctuations between 1975 and 2008 in the
18 Greater Himalaya Range of Zanskar, southern Ladakh, Journal of Mountain Sciences,
19 8, 374-389, 2011.

20 Karma, Ageta, Y., Naito, N., Iwata, S., and Yabuki, H.: Glacier distribution in the
21 Himalayas and glacier shrinkage from 1963 to 1993 in the Bhutan Himalayas, Bulletin
22 of Glaciological Research, 20, 29-40, 2003.

23 Kaser, G., Grosshauser, M., and Marzeion, B.: Contribution potential of glaciers to water
24 availability in different climate regimes, P Natl Acad Sci USA, 107, 20223-20227, Doi
25 10.1073/Pnas.1008162107, 2010.

26 Kayastha, R. B., Takeuchi, Y., Nakawo, M., and Ageta, Y.: Practical prediction of ice
27 melting beneath various thickness of debris cover on Khumbu Glacier, Nepal, using a
28 positive degree-day factor, in: Debris-Covered Glaciers, edited by: Raymond, C. F.,
29 Nakawo, M., Fountain, A., IAHS, Wallingford, UK, 71-81, 2000.

30 Krishna, A. P.: Snow and glacier cover assessment in the high mountains of Sikkim
31 Himalaya, Hydrological Processes, 19, 2375-2383, 2005.

32 Kulkarni, A. V.: Glacier inventory in the Himalaya, Natural resources management -a
33 new perspective, NNRMS, Bangalore, pp. 474-478., 1992b.

34 Kulkarni, A. V., Bahuguna, I. M., Rathore, B. P., Singh, S. K., Randhawa, S. S., Sood, R.
35 K., and Dhar, S.: Glacial retreat in Himalaya using Indian Remote Sensing satellite
36 data, Current Science, 92, 69-74, 2007.

Loibl, D. M., Lehmkuhl, F., and Grießinger, J.: Reconstructing glacier retreat since the Little Ice Age in SE Tibet by glacier mapping and equilibrium line altitude calculation, Geomorphology, 214, 22-39, doi:10.1016/j.geomorph.2014.03.018, 2014.

Manley, W. F.: Geospatial inventory and analysis of glaciers: A case study for the eastern Alaska Range, in Glaciers of Alaska, in: Satellite Image Atlas of Glaciers of the World: USGS Professional Paper 1386-K, edited by: Williams, R. S., Jr., and Ferrigno, J. G., 2008.

Mason, L. E.: Abode of Snow: A History of Himalayan Exploration and Mountaineering., Dutton, New York City, 372 pp., 1954.

Mihalcea, C., Mayer, C., Diolaiuti, G., D'Agata, C., Smiraglia, C., Lambrecht, A., Vuillermoz, E., and Tartari, G.: Spatial distribution of debris thickness and melting from remote-sensing and meteorological data, at debris-covered Baltoro glacier, Karakoram, Pakistan, Annals of Glaciology, 48, 49-57, 2008a.

Mihalcea, C. E., Brock, B. W., Diolaiuti, G. A., D'Agata, C., Citterio, M., Kirkbride, M. P., Cutler, M., and Smiraglia, C.: Using ASTER satellite and ground-based surface temperature measurements to derive supraglacial debris cover and thickness patterns on Miage Glacier (Mont Blanc Massif, Italy), Cold Regions Science and Technology, 52, 341-354, doi:10.1016/j.coldregions.2007.03.004, 2008b.

Mool, P. K., Bajracharya, S. R., Joshi, S. P., Sakya, K., and Baidya, A.: Inventory of Glaciers, Glacial Lakes and Glacial Lake Outburst Floods Monitoring and Early Warning Systems in the Hindu-Kush Himalayan region, Nepal, International Center for Integrated Mountain Development, Nepal, 2002.

Mool, P. K., and Bajracharya, S. R.: Tista Basin, Sikkim Himalaya: Inventory of Glaciers and Glacial Lakes and the Identification of Potential Glacial Lake Outburst Floods (GLOFs) Affected by Global Warming in the Mountains of Himalayan Region, International Center for Integrated Mountain Development, Kathmandu, Nepal, 145, 2003.

Narama, C., Kääb, A., Duishonakunov, M., and Abdrakhmatov, K.: Spatial variability of recent glacier area and volume changes in Central Asia using Corona (~1970), Landsat (~2000), and ALOS (~2007) optical satellite data, Global and Planetary Change, 71, 42-54, doi:10.1016/j.gloplacha.2009.08.002, 2010.

Nuimura, T., Fujita, K., Yamaguchi, S., and Sharma, R. R.: Elevation changes of glaciers revealed by multitemporal digital elevation models calibrated by GPS survey in the Khumbu region, Nepal Himalaya, 19922008, Journal of Glaciology, 58, 648-656, 2012.

Nuimura, T., Sakai, A., Taniguchi, K., Nagai, H., Lamsal, D., Tsutaki, S., Kozawa, A., Hoshina, Y., Takenaka, S., Omiya, S., Tsunematsu, K., Tshering, P., and Fujita, K.: The GAMDAM Glacier Inventory: a quality controlled inventory of Asian glaciers,

The Cryosphere Discuss, http://www.the-cryosphere-discuss.net/1/77/2007/, 8, 2799 - 2829, 2014.

Nuth, C., and Kääb, A.: Co-registration and bias corrections of satellite elevation data sets for quantifying glacier thickness change, The Cryosphere, 5, 271-290, doi:10.5194/tc-5-271-2011, 2011.

Palazzi, E., von Hardenberg, J., and Provenzale, A.: Precipitation in the Hindu-Kush Karakoram Himalaya: Observations and future scenarios, Journal of Geophysical Research: Atmospheres, 118, 85-100, 10.1029/2012jd018697, 2013.

Paterson, W. S. B.: The Physics of Glaciers, 3rd ed., Pergamon, Oxford, 480 pp., 1994.

Paul, F., Barrand, N., Berthier, E., Bolch, T., Casey, K., Frey, H., Joshi, S. P., Konovalov, V., Bris, R. L., Mölg, N., Nosenko, G., Nuth, C., Pope, A., Racoviteanu, A., Rastner, P., Raup, B., Scharrer, K., Steffen, S., and Winsvold, S.: On the accuracy of glacier outlines derived from remote sensing data, Annals of Glaciology, 54, doi:10.3189/2013AoG63A296, 2013.

Pfeffer, W. T., Arendt, A. A., Bliss, A., Bolch, T., Cogley, J. G., Gardner, A. S., Hagen, J. O., Hock, R., Kaser, G., Kienholz, C., Miles, E. S., Moholdt, G., Mölg, N., Paul, F., Radić, V., Rastner, P., Raup, B. H., Rich, J., Sharp, M. J., and Randolph_Consortium: The Randolph Glacier Inventory: a globally complete inventory of glaciers, Journal of Glaciology, 60, doi: 10.3189/2014JoG13J176, 2014.

Racoviteanu, A., Arnaud, Y., and Williams, M.: Decadal changes in glacier parameters in Cordillera Blanca, Peru derived from remote sensing, J Glaciol, 54, 499 - 510, 2008a.

Racoviteanu, A., Williams, M. W., and Barry, R.: Optical remote sensing of glacier mass balance: a review with focus on the Himalaya, Sensors, Special issue: Remote sensing of the environment, 3355-3383, doi: 10.3390/s8053355, 2008b.

Racoviteanu, A., Paul, F., Raup, B., Khalsa, S. J. S., and Armstrong, R.: Challenges and recommendations in mapping of glacier prameters from space: results of the 2008 Global Land Ice Measurements frpom Space (GLIMS) workshop, Boulder, Colorado, USA, Annals of Glaciology, 50, 53-69, 2009.

Racoviteanu, A., Armstrong, R., and Williams, M.: Evaluation of an ice ablation model to estimate the contribution of melting glacier ice to annual discharge in the Nepal Himalaya, Water Resources Research, 49, 5117 - 5133, DOI: 10.1002/wrcr.20370, 2013a.

Racoviteanu, A., Nicholson, L., and Arnaud, Y.: Surface characteristics of debris-covered glacier tongues in the Khumbu Himalaya derived from remote sensing texture analysis, European Geophysical Union (EGU) General Assembly, Vienna, Austria, 2013b.

1 Racoviteanu, A., Arnaud, Y., Bahuguna, I. M., Bajracharya, S., Berthier, E., Bhambri, R.,
2 Bolch, T., Byrne, M., Chaujar, R. K., Kääb, A., Kamp, U., Kargel, J., Kulkarni, A. V.,
3 Leonard, G., Mool, P., Frauenfelder, R., and Sossna, I.: Himalayan glaciers, in: Global
4 Land and Ice Monitoring from Space: Satellite Multispectral Imaging of Glaciers,
5 edited by: Kargel, J. S., Bishop, M. P., Kääb, A., and Raup, B. H., Springer-Praxis,
6 Heidelberg, 549-582, 2014.

7 Racoviteanu, A. E., and Williams, M. W.: Decision tree and texture analysis for mapping
8 debris-covered glaciers: a case study from Kangchenjunga, eastern Himalaya, Remote
9 Sensing Special issue, 4, 3078-3109, doi:3010.3390/rs4103078, 2012.

10 Raj, K. B. G., Remya, S. N., and Kumar, K. V.: Remote sensing-based hazard assessment
11 of glacial lakes in Sikkim Himalaya, Current Science, 104, 359-364, 2013.

12 Raup, B. H., Kääb, A., Kargel, J. S., Bishop, M. P., Hamilton, G., Lee, E., Paul, F., Rau,
13 F., Soltesz, D., Khalsa, S. J. S., Beedle, M., and Helm, C.: Remote sensing and GIS
14 technology in the Global Land Ice Measurements from Space (GLIMS) Project,
15 Computers and Geosciences, 33, 104-125, 2007.

16 GLIMS Analysis tutorial:
17 http://www.glims.org/MapsAndDocs/assets/GLIMS_Analysis_Tutorial_a4.pdf,
18 access: 04-01-2014, 2007.

19 Rees, W. G.: Remote sensing of snow and ice, Taylor & Francis Group, Boca Raton FL,
20 2003.

21 Sakai, A., Nakawo, M., and Fujita, K.: Distribution Characteristics and Energy Balance
22 of Ice Cliffs on Debris-Covered Glaciers, Nepal Himalaya, Arctic Antartcic and
23 Alpine Research, 34, 12-19, 2002.

24 Sakai, A., and Fujita, K.: Correspondence: Formation conditions of supraglacial lakes on
25 debris covered glaciers in the Himalaya, Journal of Glaciology, 56, 177-181, 2010.

26 Salerno, F., Buraschi, E., Bruccoleri, G., Tartari, G., and C.Smiraglia: Glacier surface-
27 area changes in Sagarmatha pational park, Nepal, in the second half of the 20th
28 century, by comparison of historical maps, Jounal of glaciology, 54, 738-752, 2008.

29 Salerno, F., Thakuri, S., D'Agata, C., Smiraglia, C., Manfredi, E. C., Viviano, G., and
30 Tartari, G.: Glacial lake distribution in the Mount Everest region: Uncertainty of
31 measurement and conditions of formation, Global and Planetary Change, 92-93, 30-
32 39, 2012.

33 Scherler, D., Bookhagen, B., and Strecker, M. R.: Spatially variable response of
34 Himalayan glaciers to climate change affected by debris cover, Nature Geosci, 4, 156-
35 159, http://www.nature.com/ngeo/journal/v4/n3/abs/ngeo1068.html - supplementary-
36 information, 2011.

1 Shanker, R.: Glaciological studies in India; contribution from Glaciological Survey of
2 India, in: Proceesings of Symposium on Snow, Ice and Glacier, March 1999,
3 Geological Survey of India Special Publication 53, 11-15, 2001.

4 Shrestha, A., Wake, C. P., Dibb, J. E., and Mayevski, P. A.: Precipitation fluctuations in
5 the Nepal Himalaya and its vicinity and relationship with some large-scale
6 climatologic patterns, Int J Climatol, 20, 317-327, 2000.

7 Srikantia, S. V.: Restriction on maps: A denial of valid geographic information, Current
8 Science, 79, 484-488, 2000.

9 National Map Policy:
10 http://www.surveyofindia.gov.in/tenders/nationalmappolicy/nationalmappolicy.pdf,
11 access: 2014 - 06 - 01, 2005.

12 Thakuri, S., Salerno, F., Smiraglia, C., Bolch, T., D'Agata, C., Viviano, G., and Tartari,
13 G.: Tracing glacier changes since the 1960s on the south slope of Mt. Everest (central
14 Southern Himalaya) using optical satellite imagery, The Cryosphere 8, 1297-1315,
15 doi:10.5194/tc-8-1297-2014, 2014.

16 USGS-EROS: Declassified Imagery-1, https://lta.cr.usgs.gov/declass_1, access: 02-21,
17 2015.

18 Wagnon, P., Vincent, C., Arnaud, Y., Berthier, E., Vuillermoz, E., Gruber, S., Ménégoz,
19 M., Gilbert, A., Dumont, M., and Pokharel, B.: Seasonal and annual mass balances of
20 Mera and Pokalde glaciers (Nepal Himalaya) since 2007, The Cryosphere, 7, 1769 -
21 1786, doi:10.5194/tc-7-1769-2013, 2013.

22 Wessels, R. L., Kargel, J. S., and Kieffer, H. H.: ASTER measurement of supraglacial
23 lakes in the Mount Everest region of the Himalaya, in: Annals of Glaciology, Vol 34,
24 2002, Annals of Glaciology, 399-408, 2002.

25 Yanai, M., Li, C., and Song, Z.: Seasonal heating of the Tibetan plateau and its effect on
26 the evolution of the Asian summer monsoon, J. Meteorol. Soc. Jpn, 70, 319-351, 1992.

27 Zhang, Y., Fujita, K., Liu, S., Liu, Q., and Nuimura, T.: Distribution of debris thickness
28 and its effect on ice melt at Hailuogou glacier, southeastern Tibetan Plateau, using in
29 situ surveys and ASTER imagery, Journal of Glaciology, 57, 1147-1157, 2011.

Tables

Table 1. Summary of satellite imagery used in this study

Sensor	Scene ID	Date	Spatial resolution	Image type
Corona KH4	DS009048070DA244 DS009048070DA243 DS009048070DA242	1962-10-25	7.5 m	Panchromatic
Landsat ETM+	L7CPF20001001_20001231_07	2000-12-26	15 m 28.5 m 90 m	Pancromatic Visible,shortwave Thermal infrared
ASTER	AST_L1A#003_12012000051205_07292001131755	2000-12-01		
	AST_L1A#003_12012000051214_07292001131813	2000-12-01		
	AST_L1A_00311272001045729_02222004173619	2001-11-27	15 m 30 m 90 m	Visible Shortwave Thermal infrared
	AST_L1A#00301052002050207_01302002193030	2002-01-05		
	AST_L1A#00301052002050216_01302002193046	2002-01-05		
	AST_08_00310292002045428_20101212181710_16443	2002-10-29	90 m	Surface kinetic temperature
QuickBird	1010010004BD8700 1010010004BB8F00	2006-01-01 2006-01-06	2.4 m	Visible, shortwave
WorldView-2	102001000FBA1D00 102001000586E700	2010-12-02 2009-12-01	.50 m	Panchromatic

Table 2. Spatial domains used for analysis and their characteristics

Spatial domain	Number of glaciers	Area in 2000 (km^2)	Details
1. Landsat/ ASTER	487	1463 ± 88	The entire study area extending from Sikkim to China, as well as parts of western Bhutan and eastern Nepal
2. Corona KH4	232	777 ± 46	Glaciers of eastern Nepal (Tamor basin) and Sikkim (Zemu basin)
3. QB/WV2	50	551 ± 34	Selected glaciers from the Kanchenjunga-Sikkim area

Table 3. Topographic zones in spatial domain 1

	N side (China)	W side (Nepal)	E side (Sikkim)	E side (Bhutan)
Mean basin elevation (m)	4931	4819	4658	4491
Mean rainfall TRMM (mm/yr)	146	805	977	383

Table 4. Topographic parameters for glaciers in spatial domain 1 and sub-regions based on 2000s Landsat/ASTER analysis. All parameters are presented on a) region-by-region and b) glacier-by-glacier basis from the SRTM DEM. Debris cover fraction is calculated as % glacier area of debris covered glaciers only.

Parameter	All	Nepal	Sikkim	Bhutan	China
a) Region-wide averages					
Number of glaciers	487	162	186	30	109
Glacierized area (km^2)	1463 ± 88	488 ± 29	569±34	106 ± 6	300±18
Number of debris-covered tongues	68	30	27	7	4
Debris cover area (km^2)	161±10	64±4	78±5	14±1	6±0.4
Debris cover (% total glacier area)	11	13	14	13	2
b) Glacier averages					
Minimum elevation (m)	4908	4760	4702	4926	5425
Median elevation (m)	5702	5715	5569	5652	5950
Maximum elevation (m)	6793	6928	6908	6685	6530
Slope (degree)	23	24	23	27	21
Aspect (degree)	177	236	131	134	180
Mean glacier size (km^2)	3	3	3	4	3
Length (km)	2	2	2	3	2
Thickness (m)	24	23	23	31	27
Debris cover fraction (%)	23	21	23	32	17

Table 5. Overall glacier area changes east vs. west for the 232 glaciers in spatial domain 2 from 1962 (Corona) to 2000 (Landsat/ASTER).

Sub-region	Area (km^2)		Area loss 1962 - 2000		
	1962	2000	km^2	%	% yr^{-1}
Nepal	323.9±10	269.1±16	54.8±19	16.9±6	0.44±0.2
Sikkim	634.7±19	507.0±35	127.7±42	20.1±8	0.52±0.2
All spatial domain	958.7±31	776.1±47	182.5±40	19.0±4	0.50±0.1

Table 6. Glacier area change for debris-covered versus clean glaciers in spatial domain 2 from 1962 to 2000. Change is shown as percent of glacier area on a glacier-by-glacier basis.

Glacier type/ Sub-region	Sikkim		Nepal		All	
	Number of glaciers	Area loss (%)	Number of glaciers	Area loss (%)	Number of glaciers	Area loss (%)
Clean glaciers	144	34.7	53	31.6	197	33.9
Debris-covered glaciers	20	20.8	15	23.8	35	22.1
Both types	164	33.0	68	29.9	232	32.1

Table 7 Linear regression of area change on topographic and climatic variables for the 232 glaciers in the spatial domain 2

Regression	Coefficient	P-value
Glacier area	-0.47	0.0003**
Altitudinal range	-0.01	<0.001**
Minimum elevation	0.008	0.02*
Median elevation	-0.01	0.001**
Maximum elevation	-0.01	<0.001**
Percent debris	-0.004	0.83
Slope	0.47	0.01*
Aspect	0.03	0.007**
Solar radiation	0.01	0.74
Precipitation	-0.002	0.26

* Significant at the 0.05 level (2-tailed).
** Significant at the 0.01 level (2-tailed).

Table 8. Comparison of glacier parameters for clean glaciers versus debris-covered glaciers in spatial domain 2.

Parameter	Clean glaciers	Debris-covered glaciers
Area (km^2)	1.2	15.0
Area change (%)	33.9	22.1
Slope	25.8	24.5
Minimum elevation (m)	5105.6	4714.2
Median elevation (m)	5424.5	5538.9
Altitudinal range (m)	627.6	1928.6
Length (km)	1.3	6.7

Table 9 Glacier area change in Sikkim based on previous studies. The percent area change is given with respect to the 1962 Corona glacier inventory from this study.

Study	Year	Data source	Number of glaciers	Area (km^2)	Area change since 1960s	
					%	% yr^{-1}
This study	1962	Corona KH4	178	658±20	-	-
Geological Survey of India (1999)	~1960 -1970s	Indian 1:63,000 topographic maps	449	706	+7.3	+0.9
Kulkarni and Narain (1990)	1987/ 1989	IRS-1C satellite images	n/a	426	-35.0	-1.4
ICIMOD Mool et al, (2002)	2000	Landsat TM, IRS-1C, topographic maps	285	577	-11.4	-0.3
This study	2000	Landsat TM, ASTER	185	569 ±34	-13.5 ±6.4	-0.3 ±0.1

List of figures

Figure 8 Dependency of glacier area change 1962 – 2000 on a) glacier altitudinal range (maximum – minimum elevation) and b) glacier area. Debris-covered glaciers are shown as grey solid circles; clean glaciers are shown as black solid triangles.

Figure 9 Distribution of surface temperatures along longitudinal for selected debris-covered tongues in spatial domain 2. Temperatures are extracted from ASTER kinetic temperature data (AST08) from the Oct 29th, 2002 image.

Figure 10 Surface temperature distribution along longitudinal transects from selected glaciers. Distance is measured from the upper part of the debris-covered area down glacier to the terminus. Labels point to: A- Kanchenjunga glacier, B- Yalung glacier and C- Zemu glacier.

Figure 11 Area changes for some glaciers in the Zema Chhu basin Sikkim from 1962 to 2006: a) 1962 Corona-based glacier outlines (in blue) and b) 2006 QB glacier outlines (in orange).

Figure 12 Close-up view of glacier area changes around the N. and S. Lhonak glaciers 1962 to 2006, showing changes in the pro-glacial lakes.

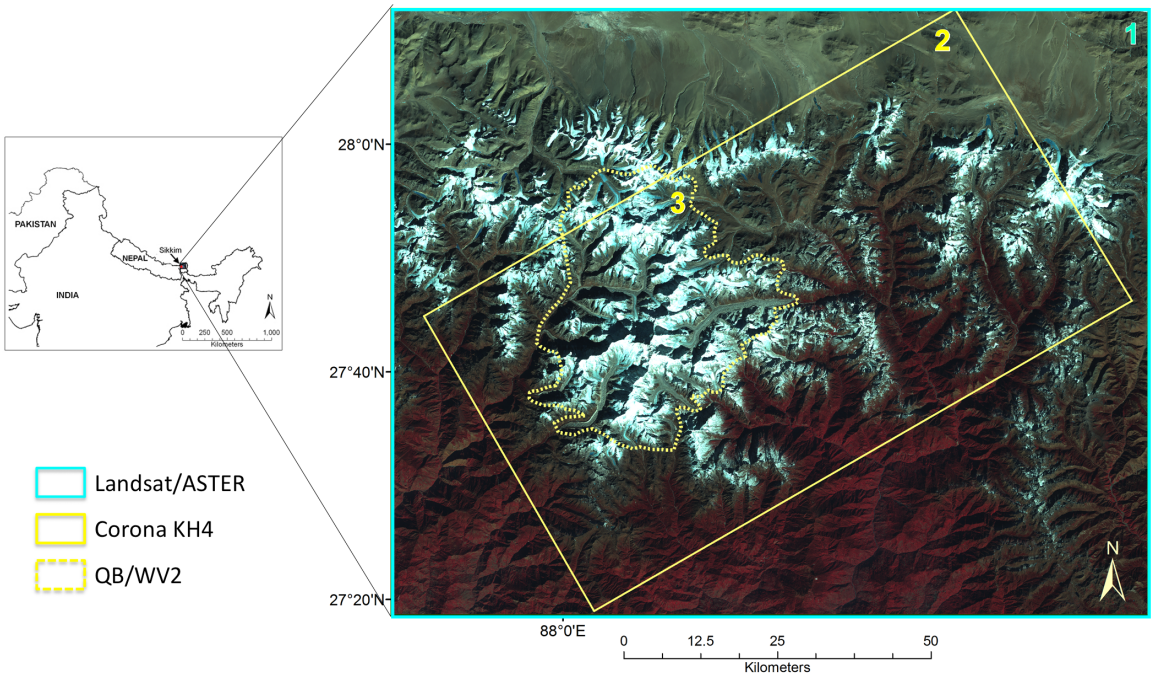
PAKISTAN
NEPAL
Sikkim
INDIA
0 250 500 1,000
Kilometers
N
Landsat/ASTER
Corona KH4
QB/WV2
28°0'N
27°40'N
27°20'N
88°0'E
1
2
3
N
0 12.5 25 50
Kilometers

Figure 1

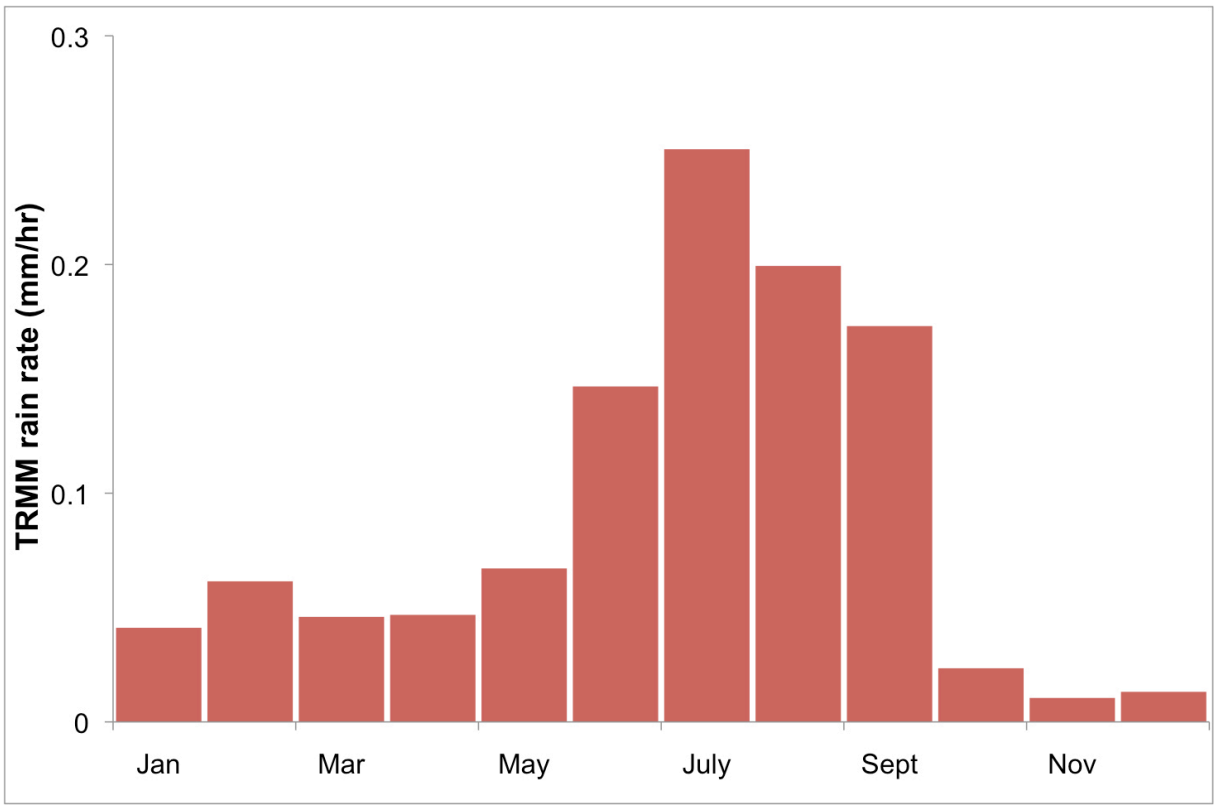

Figure 2

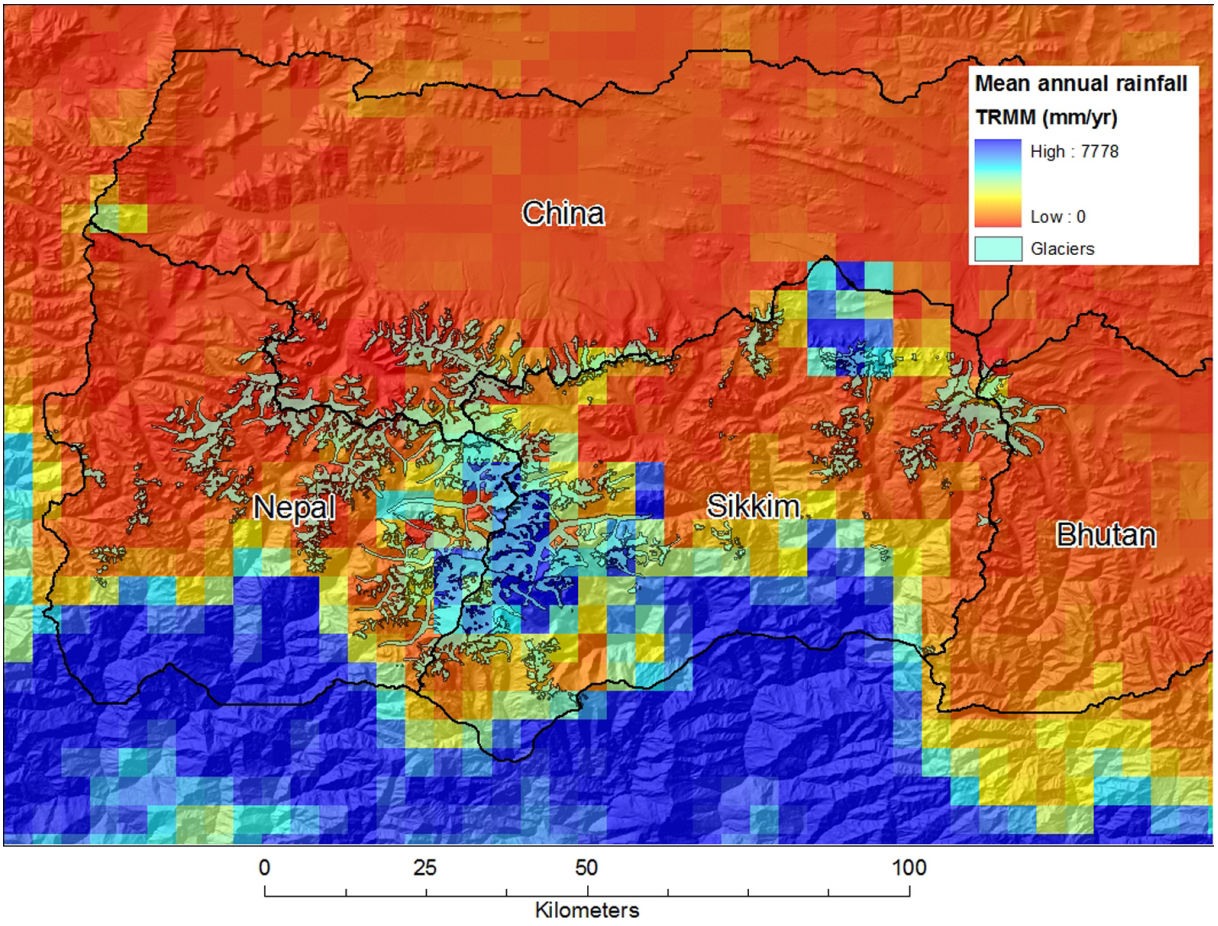
Mean annual rainfall
TRMM (mm/yr)
High : 7778
Low : 0
Glaciers
China
Nepal
Sikkim
Bhutan
0
25
50
100
Kilometers

Figure 3

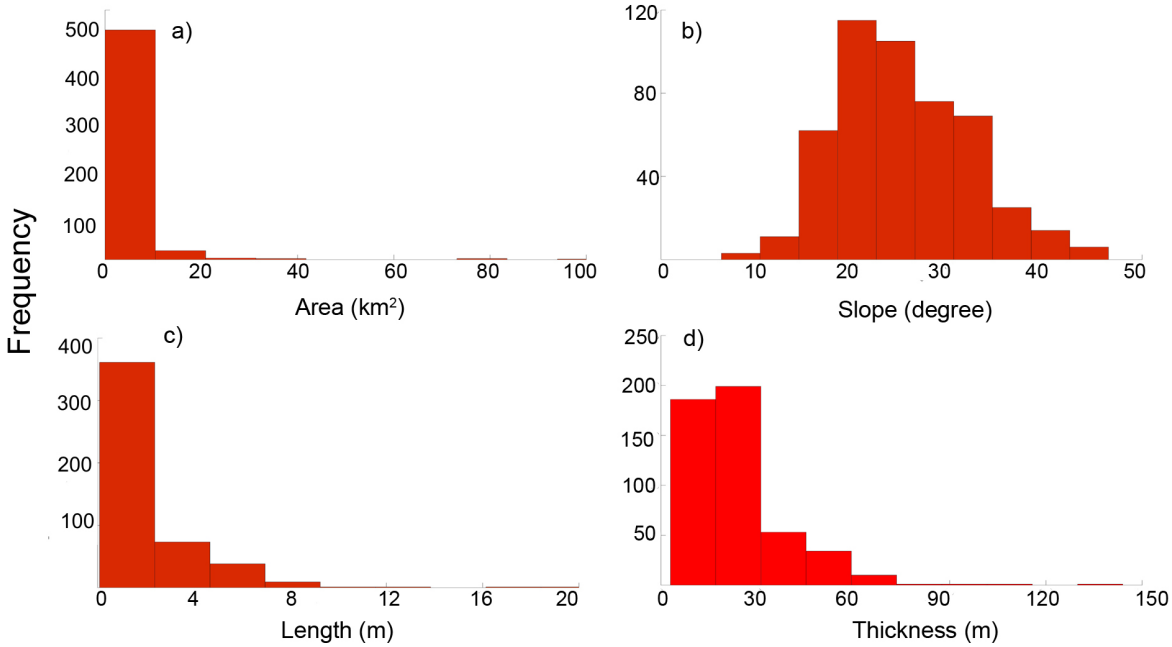
a)
b)
c)
d)
Frequency
Area (km²)
Slope (degree)
Length (m)
Thickness (m)
500
400
300
200
100
0
20
40
60
80
100
120
80
40
0
10
20
30
40
50
400
300
200
100
0
4
8
12
16
20
250
200
150
100
50
0
30
60
90
120
150

Figure 4

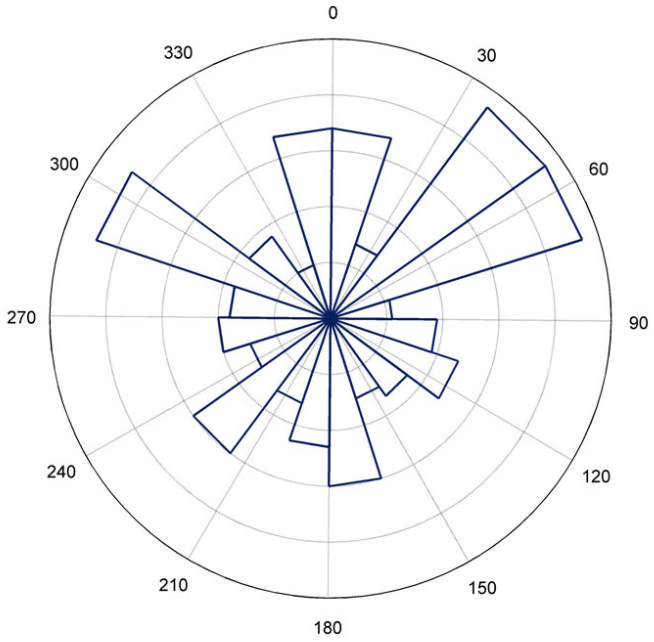

Figure 5

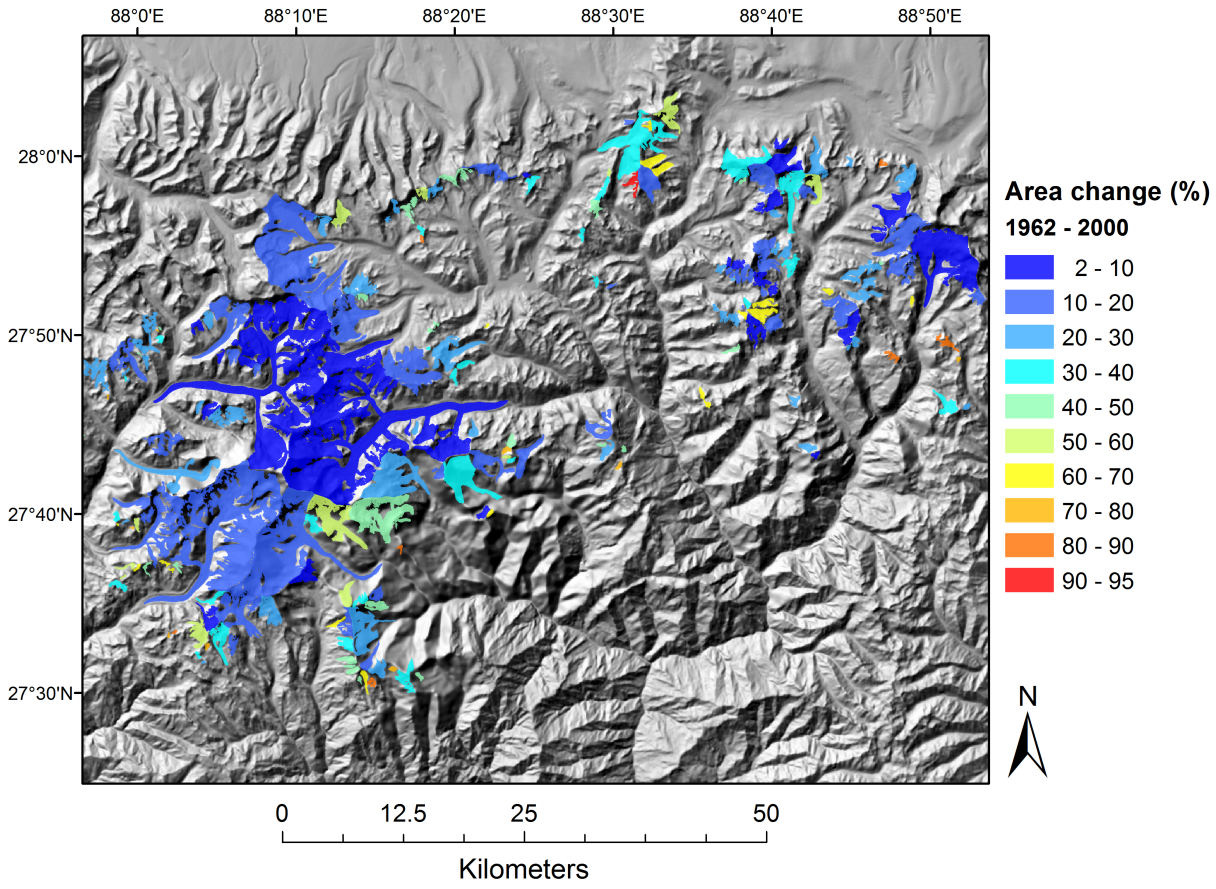
88°0'E
88°10'E
88°20'E
88°30'E
88°40'E
88°50'E
28°0'N
27°50'N
27°40'N
27°30'N
Area change (%)
1962 - 2000
2 - 10
10 - 20
20 - 30
30 - 40
40 - 50
50 - 60
60 - 70
70 - 80
80 - 90
90 - 95
N
0
12.5
25
50
Kilometers

Figure 6

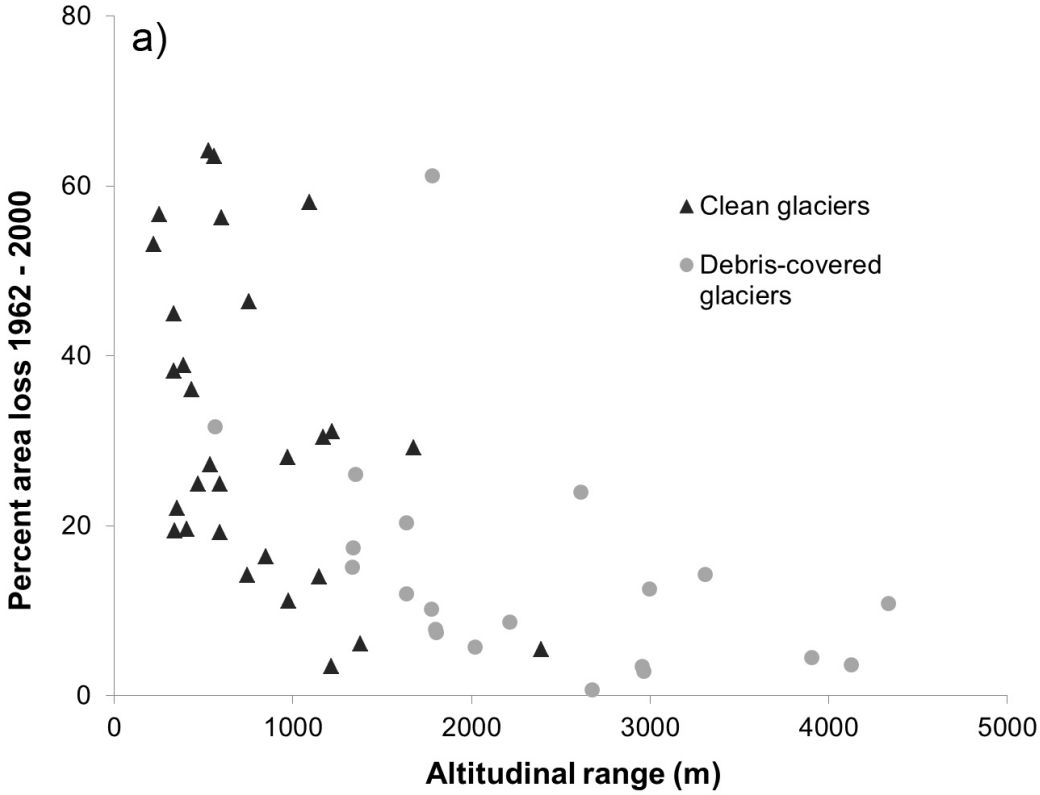
a)
Percent area loss 1962 - 2000
Altitudinal range (m)
Clean glaciers
Debris-covered glaciers
0
20
40
60
80
0
1000
2000
3000
4000
5000

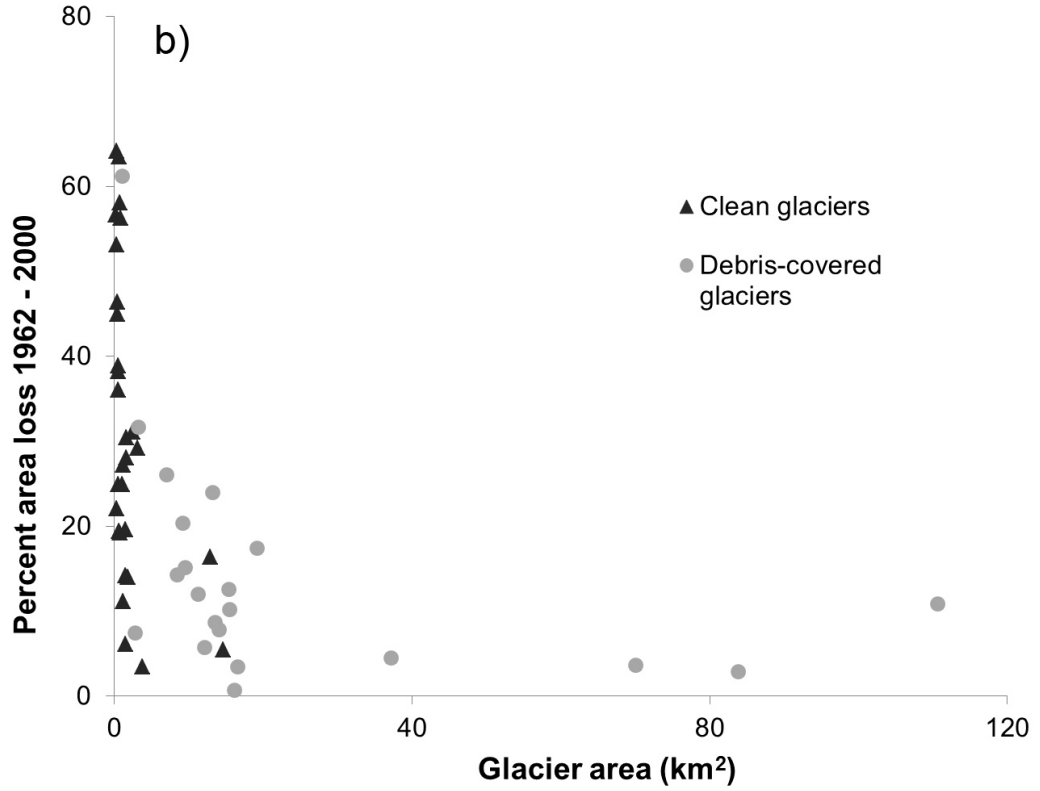
b)
Percent area loss 1962 - 2000
Glacier area (km²)
Clean glaciers
Debris-covered glaciers
0
20
40
60
80
0
40
80
120

Figure 7

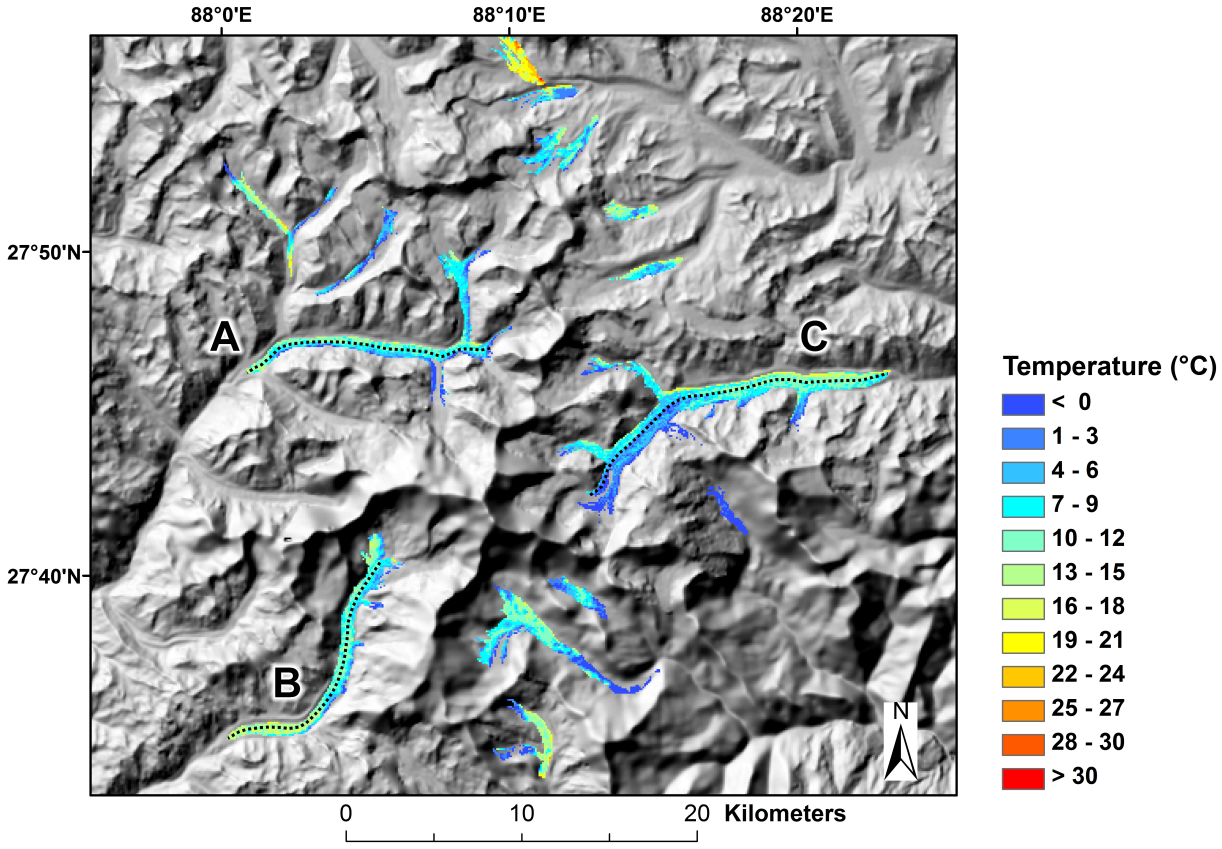
88°0'E
88°10'E
88°20'E
27°50'N
27°40'N
A
B
C
N
0
10
20
Kilometers
Temperature (°C)
< 0
1 - 3
4 - 6
7 - 9
10 - 12
13 - 15
16 - 18
19 - 21
22 - 24
25 - 27
28 - 30
> 30

Fig. 8

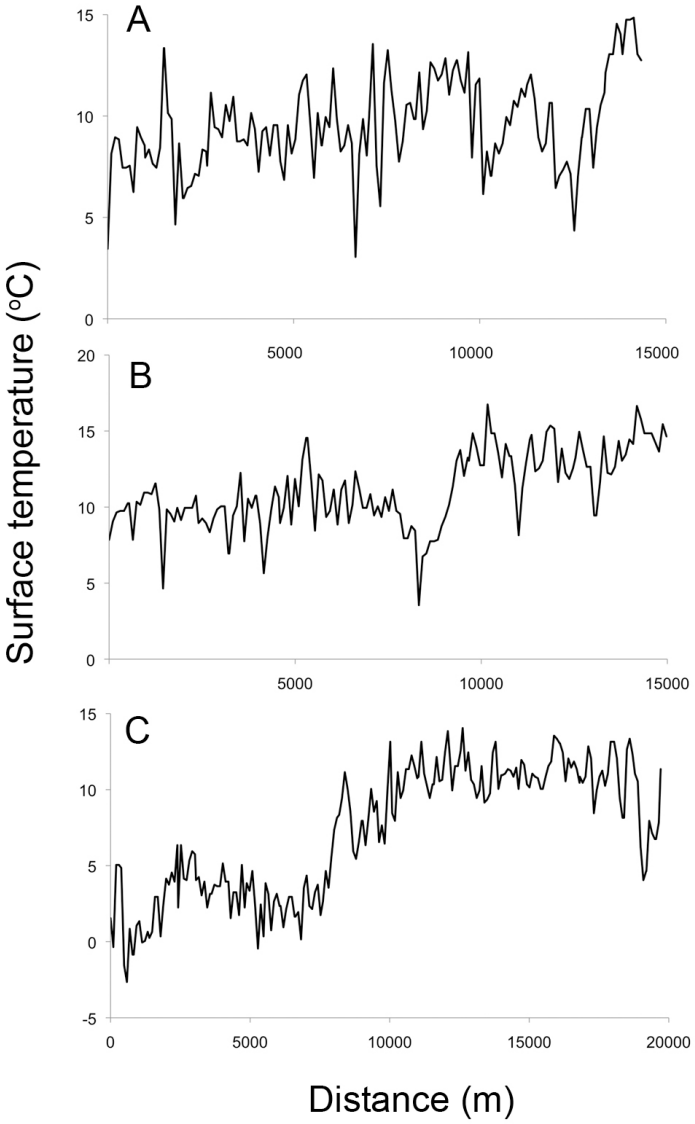
A
B
C
Surface temperature (°C)
Distance (m)
15
10
5
0
20
-5
5000
10000
15000
20000

Figure 9

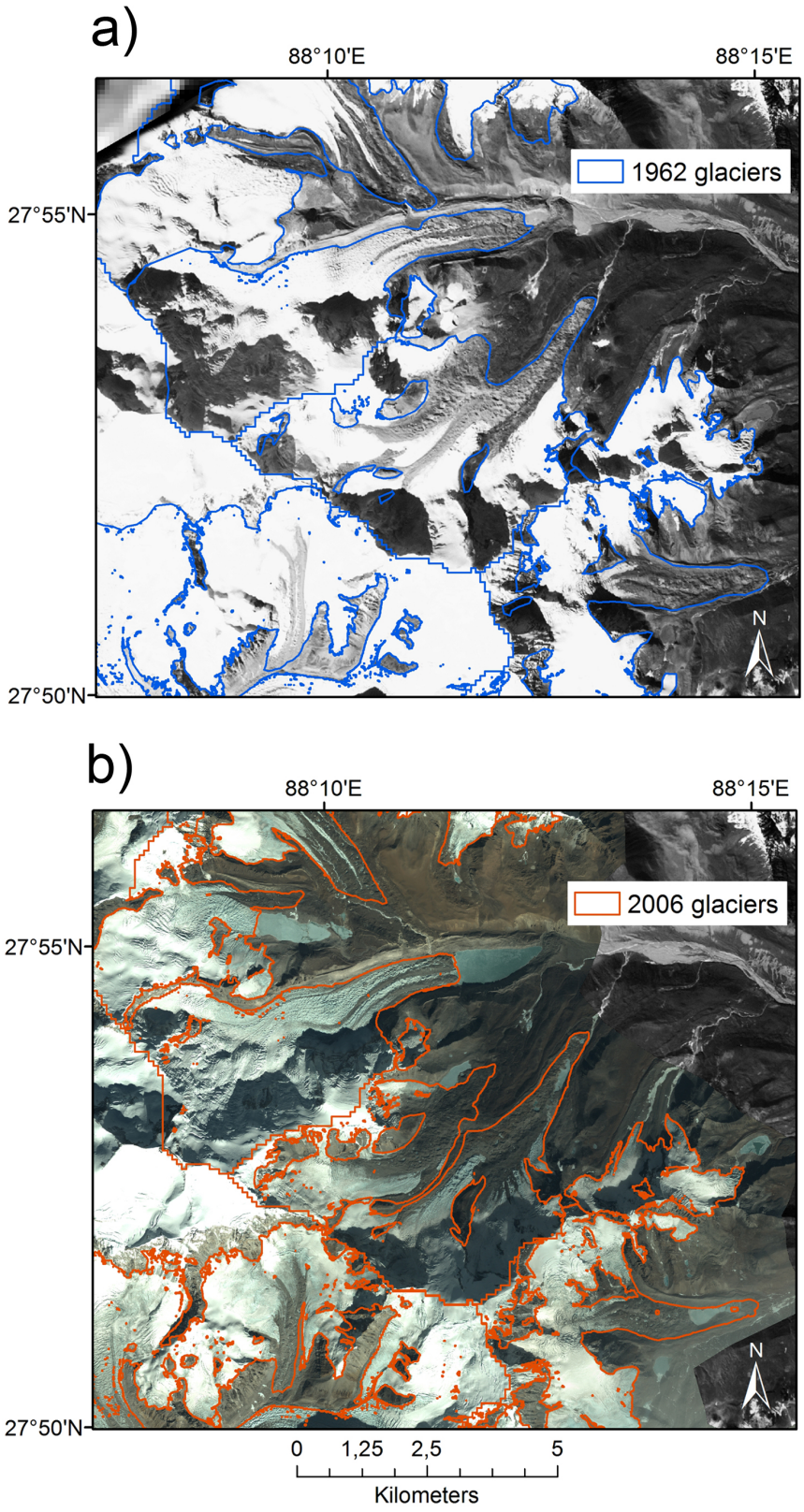
a)
88°10'E
88°15'E
27°55'N
27°50'N
1962 glaciers
N
b)
88°10'E
88°15'E
27°55'N
27°50'N
2006 glaciers
N
0
1,25
2,5
5
Kilometers

Figure 10

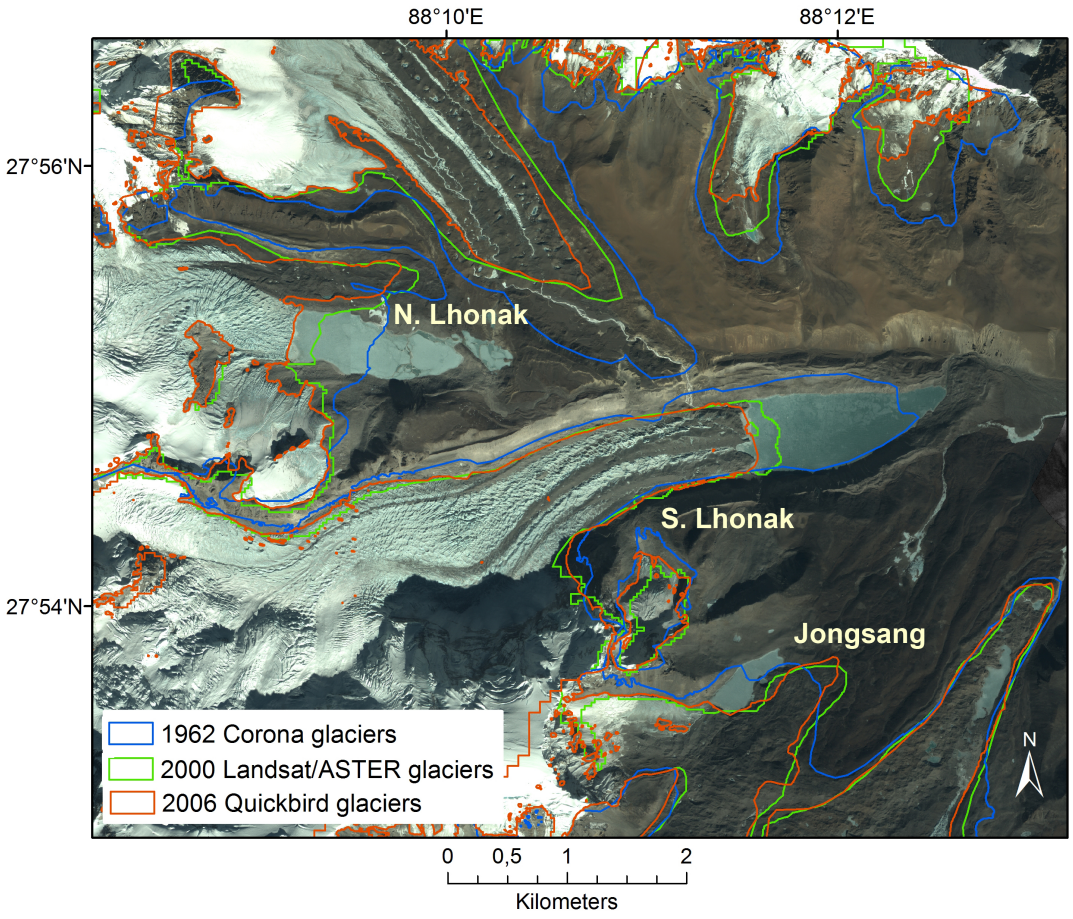
88°10'E
88°12'E
27°56'N
27°54'N
N. Lhonak
S. Lhonak
Jongsang
1962 Corona glaciers
2000 Landsat/ASTER glaciers
2006 Quickbird glaciers
N
0
0,5
1
2
Kilometers

Figure 11